Full counting statistics, fluctuation relations, and linear response properties in a one-dimensional Kitaev chain

Fan Zhang [1], Jiayin Gu [2], and H. T. Quan [1,3,4,*]

[1]*School of Physics, Peking University, Beijing 100871, China*
[2]*School of Physics and Technology, Nanjing Normal University, Nanjing 210023, People's Republic of China*
[3]*Collaborative Innovation Center of Quantum Matter, Beijing 100871, China*
[4]*Frontiers Science Center for Nano-optoelectronics, Peking University, Beijing, 100871, China*

(Received 25 July 2022; revised 16 November 2022; accepted 10 July 2023; published 7 August 2023)

We analytically calculate the cumulant generating function of energy and particle transport in an open one-dimensional Kitaev chain at finite temperature by utilizing the Keldysh technique. The joint distribution of particle and energy currents satisfies different fluctuation relations in different regions of the parameter space as a result of U(1) symmetry breaking and energy conservation. Furthermore, we investigate the linear response behavior of the Kitaev chain within the framework of three-terminal systems, deriving the expressions for the Seebeck coefficient and thermal conductance. Notably, we observe a pronounced peak in the thermal conductance near the phase transition point, in agreement with previous predictions. Additionally, we prove that the peak value saturates at half of the thermal conductance quantum for finite-length chains at the zero temperature limit.

DOI: 10.1103/PhysRevE.108.024110

I. INTRODUCTION

Microreversibility, which is a fundamental symmetry of the physical laws, imposes remarkable constraints on the nonequilibrium dynamics of a system. The most famous example is the celebrated Onsager-Casimir reciprocal relation, which states that the matrix of linear kinetic coefficient is symmetric [1–3]. This relation greatly reduces the number of response coefficients in a transport process, thus finding wide applications in transport experiments. Another example is the fluctuation-dissipation relation (FDR), which relates the dissipation or response in a nonequilibrium process to the properties in equilibrium [4]. Recently, a new family of nonequilibrium relations, called *fluctuation relations* (FRs), have been discovered [5–15]. The derivation of the FRs only relies on the microreversibility of the system and does not depend on the microscopic details. These FRs generalize the above two well-known relations from the linear-response regime to regimes arbitrarily far away from equilibrium. From these relations, one can not only easily reproduce the results in linear response theory such as the Green-Kubo formula, but also obtain relations of higher-order response coefficients [16–23].

The most general form of a FR about the entropy production in an open system can be written as

$$\frac{P(\Delta\Omega)}{P(-\Delta\Omega)} = e^{\Delta\Omega},$$

where $P(\Delta\Omega)$ is the probability distribution of entropy production $\Delta\Omega$. According to principles of thermodynamics, one can relate $\Delta\Omega$ to various physical observables, such as particle number, exchanged heat, and applied work. In an open system without driving, there is no work done on the system. The entropy production is associated with the exchange of particles and energy; the corresponding FR is termed as exchange FR [24].

In the derivation of exchange FR, two ingredients are used. One is the microreversibility of the equation of motion and the other is the particle and energy conservation. Whereas the former is well recognized, the latter is implicit and taken for granted since the conservation law is a result of U(1) symmetry and time-translation symmetry. However, in condensed matter physics, the U(1) symmetry can be explicitly broken in some systems described by low-energy effective Hamiltonian, such as the BCS Hamiltonian of the superconductor. The breaking of U(1) symmetry implies that the particle number is not conserved in the transport process, and it can lead to new forms of exchange FR.

In a previous work [25], we show that the exchange FR of particle current in the one-dimensional (1D) Kitaev chain in the steady state takes various forms for different parameters. It is due to the presence of a pairing term such as $\Delta\hat{c}^{\dagger}_{j+1}\hat{c}^{\dagger}_{j}$ which explicitly breaks U(1) symmetry. The competition between the pairing potential, the hopping amplitude, and the chemical potential gives rise to different microscopic transport processes, namely, the normal transport (NT), the local Andreev reflection (LAR), and the crossed Andreev reflection (CAR). Each particle current component satisfies a steady-state FR.

In this article, we go one step further and study the joint probability distribution of energy and particle transport. We use the Keldysh technique to analytically calculate the full counting statistics (FCS) of the particle and energy currents. It is shown that the joint distribution of particle and energy

*Corresponding author: htquan@pku.edu.cn

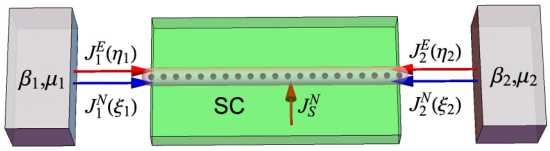

FIG. 1. The setup of an open Kitaev chain. A nanowire is put above an grounded s-wave superconductor (SC) and is coupled to two reservoirs. The left and right reservoirs are labeled as $\alpha = 1, 2$. The temperature and chemical potential for reservoir 1 (2) are β_1, μ_1 (β_2, μ_2), respectively. The nonzero affinities drive the system into a steady state in the long-time limit. There are five currents: two energy currents J_1^E, J_2^E (red arrow) associated with the counting fields η_1, η_2, two particle currents J_1^N, J_2^N (blue arrow) associated with the counting fields ξ_1, ξ_2, and a supercurrent J_S^N from the SC to the nanowire.

currents obeys different exchange FRs due to U(1) symmetry breaking and energy conservation. As an application of the FCS, we study the linear response of the Kitaev chain at finite temperature and reproduce the well-know quantized electrical conductance and the half quantized thermal conductance.

Our paper is structured as follows. We introduce the open 1D Kitaev chain model and analytically calculate its full counting statistics of energy and particle in Sec. II. We discuss the exchange FR in Sec. III. In Sec. IV, we study the linear response properties of the Kitaev chain. In Sec. V, we discuss our results and make a summary.

II. MODEL AND FULL COUNTING STATISTICS

We consider a Kitaev chain connected to two reservoirs. The set up is shown in Fig. 1. A nanowire is put above an s-wave superconductor (SC) and coupled to two reservoirs. Due to the proximity effect, the Cooper pairs can leak into the nanowire, and turns the low-energy effective Hamiltonian of the nanowire into a 1D Kitaev chain [26–28]. This hybrid system has been an canonical platform in experiment in the search of Majorana zero modes (MZMs), and a convincing signature of MZMs is yet to be confirmed [28–35]. The whole Hamiltonian is

$$\hat{H} = \hat{H}_{\rm K} + \sum_{\alpha=1,2} \hat{H}_\alpha + \hat{H}_{\rm I}, \tag{1}$$

where the Hamiltonian of the Kitaev chain is

$$\hat{H}_{\rm K} = -\mu \sum_{j=1}^{N} \left(\hat{c}_j^\dagger \hat{c}_j - \frac{1}{2}\right) + \sum_{j=1}^{N-1} (-t\, \hat{c}_j^\dagger \hat{c}_{j+1} + \Delta\, \hat{c}_j \hat{c}_{j+1} + \text{H.c.}), \tag{2}$$

with μ, t, Δ the chemical potential, the hopping amplitude and the superconducting gap. The Hamiltonian of the SC and the interaction between the SC and the nanowire is completely traced out and their effect is captured by the superconducting gap Δ. The operator $\hat{c}_j^\dagger$ ($\hat{c}_j$) creates (annihilates) an electron on site j; N is the site number of the Kitaev chain. The reservoirs are described by free fermions

$$\hat{H}_\alpha = \sum_j (\hbar\omega_{\alpha j} - \mu_\alpha)\hat{c}_{\alpha j}^\dagger \hat{c}_{\alpha j}, \quad \alpha = 1, 2. \tag{3}$$

Here, $\omega_{\alpha j}$ denotes the energy of the jth state of reservoir α of which the chemical potential is μ_α. We assume linear couplings between the Kitaev chain and the reservoirs

$$\hat{H}_{\rm I} = \sum_j \lambda_{1j}(\hat{c}_{1j}^\dagger \hat{c}_1 + \hat{c}_1^\dagger \hat{c}_{1j}) + \sum_j \lambda_{2j}(\hat{c}_{2j}^\dagger \hat{c}_N + \hat{c}_N^\dagger \hat{c}_{2j}), \tag{4}$$

with $\lambda_{\alpha j}$ the coupling strength. In experiment, the chemical potential μ and the superconducting gap Δ are controlled by the so-called "super gate" and an external magnetic field, respectively [35,36]. The coupling strengths $\lambda_{\alpha j}$ are tuned by altering the barrier gate settings. We will use the hopping amplitude t as the unit of energy and set $\hbar = 1$ without loss of generality.

We adopt the two-point measurement scheme. We assume that the initial state is a product state, and every part is prepared in its thermal equilibrium state $\hat{\rho}_0 = e^{-\beta_0 \hat{H}_{\rm K} - \sum_{\alpha=1,2} \beta_\alpha \hat{H}_\alpha}/\text{Tr}[e^{-\beta_0 \hat{H}_{\rm K} - \sum_{\alpha=1,2} \beta_\alpha \hat{H}_\alpha}]$, where β_0 and β_α are the initial temperatures of the Kitaev chain and reservoir α, respectively. We measure the particle number $\hat{N}_\alpha = \sum_j \hat{c}_{\alpha j}^\dagger \hat{c}_{\alpha j}$ and the energy $\hat{H}_\alpha$ of reservoir α simultaneously at the initial time and a latter time τ. The outcomes are $E_{\alpha k}$, $N_{\alpha k}$ at the initial time and $E'_{\alpha j}$, $N'_{\alpha j}$ at the final time. The particle (energy) exchanged between the reservoir and the chain during the time interval $[0, \tau]$ is defined to be the difference between the two outcomes

$$\Delta E_{\alpha,jk} = E'_{\alpha j} - E_{\alpha k},$$
$$\Delta N_{\alpha,jk} = N'_{\alpha j} - N_{\alpha k}.$$

The joint probability distribution of observing these outcomes is given by

$$P(\Delta N_\alpha, \Delta E_\alpha) = \prod_\alpha \sum_{jk} \delta[\Delta E_\alpha - \Delta E_{\alpha,jk}]\delta[\Delta N_\alpha - \Delta N_{\alpha,jk}] \times \text{Tr}[\Pi_{1j}\Pi_{2j}\hat{U}(\tau)\Pi_{1k}\Pi_{2k}\hat{\rho}_0\Pi_{2k}\Pi_{1k}\hat{U}^\dagger(\tau)], \tag{5}$$

where $\Pi_{\alpha j}$ projects reservoir α to the eigenstate with energy $E_{\alpha j}$ and particle number $N_{\alpha j}$, and $\hat{U}(\tau)$ is the unitary evolution operator of the total Hamiltonian. For later convenience, we rewrite the stochastic variables into a compact form,

$$\Delta \boldsymbol{X} = (\Delta N_1, \Delta N_2, \Delta E_1, \Delta E_2) = (\Delta \boldsymbol{N}, \Delta \boldsymbol{E}),$$

and define the operator $\hat{\boldsymbol{X}} = (\hat{N}_1, \hat{N}_2, \hat{H}_1, \hat{H}_2)$. In practice, it is more convenient to calculate the so-called moment generating function (MGF) which encodes the same information as $P(\Delta \boldsymbol{X})$ and is defined as the Fourier transform of the joint probability distribution $P(\Delta \boldsymbol{X})$

$$Z(\boldsymbol{\lambda}) = \int d\Delta \boldsymbol{X}\; P(\Delta \boldsymbol{X}) e^{i\Delta \boldsymbol{N}\cdot\boldsymbol{\xi}} e^{i\Delta \boldsymbol{E}\cdot\boldsymbol{\eta}} = \text{Tr}[\hat{\rho}_0 \hat{U}^\dagger(\tau, 0) e^{i\hat{\boldsymbol{X}}\cdot\boldsymbol{\lambda}} \hat{U}(\tau, 0) e^{-i\hat{\boldsymbol{X}}\cdot\boldsymbol{\lambda}}], \tag{6}$$

with the counting fields $\boldsymbol{\lambda} = (\boldsymbol{\xi}, \boldsymbol{\eta}) = (\xi_1, \xi_2, \eta_1, \eta_2)$.

We insert fermionic coherent states and write it in the form of contour functional integral; by utilizing the Keldysh technique [25,37,38], we obtain the MGF of the open Kitaev chain in the long time limit $\tau \to \infty$,

$$Z(\boldsymbol{\lambda}) = \prod_{\omega} \sqrt{Z(\boldsymbol{\lambda};\omega)}, \tag{7}$$

where the MGF of every mode ω is composed of three components: the normal transport, the crossed Andreev reflection, and the local Andreev reflection

$$Z(\boldsymbol{\lambda};\omega) = \frac{Z_{\rm NT}(\xi_1-\xi_2) + Z_{\rm CAR}(\xi_1+\xi_2) + Z_{\rm LAR}(\xi_1,\xi_2)}{Z_{\rm NT}(0) + Z_{\rm CAR}(0) + Z_{\rm LAR}(0)}. \tag{8}$$

The three components are given by

$$\begin{aligned}
Z_{\rm NT}(\xi_1-\xi_2) &= p_{\rm NT}\{1+\mathcal{T}_{\rm NT}[n_{1e}\bar{n}_{2e}(e^{i(\xi_1-\xi_2)}e^{i\omega\eta_-}-1)+\bar{n}_{1e}n_{2e}(e^{-i(\xi_1-\xi_2)}e^{-i\omega\eta_-}-1)]\}\\
&\quad\times\{1+\bar{\mathcal{T}}_{\rm NT}[n_{1h}\bar{n}_{2h}(e^{-i(\xi_1-\xi_2)}e^{i\omega\eta_-}-1)+\bar{n}_{1h}n_{2h}(e^{i(\xi_1-\xi_2)}e^{-i\omega\eta_-}-1)]\},\\
Z_{\rm CAR}(\xi_1+\xi_2) &= p_{\rm CAR}\{1+\mathcal{T}_{\rm CAR}[n_{1e}\bar{n}_{2h}(e^{i(\xi_1+\xi_2)}e^{i\omega\eta_-}-1)+\bar{n}_{1e}n_{2h}e^{-i(\xi_1+\xi_2)}e^{-i\omega\eta_-}-1)]\}\\
&\quad\times\{1+\bar{\mathcal{T}}_{\rm CAR}[n_{1h}\bar{n}_{2e}(e^{-i(\xi_1+\xi_2)}e^{i\omega\eta_-}-1)+\bar{n}_{1h}n_{2e}(e^{i(\xi_1+\xi_2)}e^{-i\omega\eta_-}-1)]\},\\
Z_{\rm LAR}(\xi_1,\xi_2) &= p_{\rm LAR}\{1+\mathcal{T}_{\rm LAR,1}[n_{1e}\bar{n}_{1h}(e^{2i\xi_1}-1)+\bar{n}_{1e}n_{1h}(e^{-2i\xi_1}-1)]\}\\
&\quad\times\{1+\mathcal{T}_{\rm LAR,2}[n_{2e}\bar{n}_{2h}(e^{2i\xi_2}-1)+\bar{n}_{2e}n_{2h}(e^{-2i\xi_2}-1)]\}.
\end{aligned} \tag{9}$$

Here for simplicity, we eliminate the redundancy of the counting fields of energy by introducing a new counting field $\eta_- = \eta_1 - \eta_2$. The Fermi distribution of electrons and holes in reservoir α are denoted by $n_{\alpha e}(\omega) = f_\alpha(\omega-\mu_\alpha)$ and $n_{\alpha h}(\omega) = f_\alpha(\omega+\mu_\alpha)$, respectively, where $f_\alpha(\omega) = 1/[e^{\beta_\alpha\omega}+1]$. The unoccupied distributions are defined as $\bar{n}_{\alpha e}(\omega) \equiv 1 - n_{\alpha e}(\omega)$ and $\bar{n}_{\alpha h}(\omega) \equiv 1 - n_{\alpha h}(\omega)$. The factors $\mathcal{T}_{\rm NT}$, $\mathcal{T}_{\rm CAR}$, and $\mathcal{T}_{\rm LAR}$ ($p_{\rm NT}$, $p_{\rm CAR}$, and $p_{\rm LAR}$) are the transmission coefficients (weights) of the NT, CAR, and LAR channels, respectively, and $\bar{\mathcal{T}}(\omega) \equiv \mathcal{T}(-\omega)$. The weights are normalized $p_{\rm NT} + p_{\rm CAR} + p_{\rm LAR} = 1$. The expressions of these factors by Green's function are given in Appendix A. This form of MGF is valid for arbitrary number of sites and arbitrary parameters. Different numbers of sites correspond to different weights $p_{\rm NT}, p_{\rm CAR}, p_{\rm LAR}$ and coefficients $\mathcal{T}_{\rm NT}, \mathcal{T}_{\rm CAR}, \mathcal{T}_{\rm LAR}$ but do not affect the remaining expressions of the MGF. We also note that either only one channel is present, or all three channels are present. To see this, let us assume that only NT and CAR are present. Then an electron in the left reservoir can be reflected as an hole in the same reservoir by successively getting through the NT channel and the CAR channel $1e \xrightarrow{\rm NT} 2e \xrightarrow{\rm CAR} 1h$. In the following, we will only use η_- as the counting field for energy flow, i.e., $\boldsymbol{\eta} = \eta_-$. The reduction of the number of counting fields of energy is a consequence of energy conservation. Please note that the information of the initial state of the Kitaev chain is lost in the long-time limit.

III. FLUCTUATION RELATION

From the explicit form of MGF, we observe that the transport process is composed of independent bidirectional processes of mode ω. Every process consists of three subprocesses. The three subprocesses are the NT, the CAR, and the LAR. The NT corresponds to transferring one electron (hole) from the left reservoir to the right reservoir, while the CAR corresponds to a process in which an incoming electron from the left reservoir is turned into an outgoing hole in the right reservoir [39,40]. As a result, one electron from each reservoir is injected into the SC to form a Cooper pair. The LAR corresponds to the process in which an incident electron from one reservoir is converted into a backscattered hole. The CAR and LAR break the particle conservation in two reservoirs, which is due to the presence of a nonzero pairing potential Δ. If we take $\Delta = 0$, then $\mathcal{T}_{\rm CAR}$ and $\mathcal{T}_{{\rm LAR},\alpha}$ vanish and only $\mathcal{T}_{\rm NT}$ is nonzero. In this case, the number of conservation law recovers to two and only two counting fields $\xi_1 - \xi_2$, η_- are required to generate the cumulants of the currents. However, the particle conservation is also recovered if we take into account the third reservoir, the superconductor, which does not appear explicitly in the Hamiltonian of the open Kitaev chain.

From Eqs. (8) and (9), one can find that the MGF satisfies a symmetry relation

$$Z(\boldsymbol{\xi},\eta_-) = Z(-\boldsymbol{\xi}+i\boldsymbol{A}_N, -\eta_- + iA_E), \tag{10}$$

where $\boldsymbol{A}_N = (\beta_1\mu_1, \beta_2\mu_2)$ and $A_E = \beta_2 - \beta_1$ are the affinities. The symmetry of the MGF implies an exchange FR of the joint probability distribution [12,13,18]

$$\frac{P(\Delta N_1, \Delta N_2, \Delta E_1)}{P(-\Delta N_1, -\Delta N_2, -\Delta E_1)} = e^{\Delta N_1\mu_1\beta_1 + \Delta N_2\mu_2\beta_2} e^{\Delta E_1(\beta_2-\beta_1)}. \tag{11}$$

Under certain conditions, one of the three current components dominates the transport process and Eq. (11) is reduced to a simpler FR. We consider three different cases in the following.

The first case is when the pairing potential $\Delta = 0$, i.e., the Kitaev chain is a conventional conductor. The transmission amplitudes of CAR $\mathcal{T}_{\rm CAR}$ and LAR $\mathcal{T}_{{\rm LAR},1}, \mathcal{T}_{{\rm LAR},2}$ vanish. Whenever one reservoir receives a particle, the other reservoir

loses a particle, $\Delta N_1 = -\Delta N_2$. The FR reads

$$\frac{P(\Delta N_1, \Delta E_1)}{P(-\Delta N_1, -\Delta E_1)} = e^{\Delta N_1(\mu_1\beta_1 - \mu_2\beta_2)} e^{\Delta E_1(\beta_2 - \beta_1)}, \tag{12}$$

which is the conventional FR of two terminal systems.

If we introduce a nonzero pairing potential $\Delta \neq 0$ and turn off the hopping term $t = 0$, then only CAR will occur [41]. In this case, $\Delta N_1 = \Delta N_2$, and the FR becomes

$$\frac{P(\Delta N_1, \Delta E_1)}{P(-\Delta N_1, -\Delta E_1)} = e^{\Delta N_1(\mu_1\beta_1 + \mu_2\beta_2)} e^{\Delta E_1(\beta_2 - \beta_1)}. \tag{13}$$

Two points are worth emphasizing. The first one is that when we apply symmetric bias, i.e., $\mu_1\beta_1 = -\mu_2\beta_2$, the probability distribution $P(\Delta N_1)$ is symmetric about $\Delta N_1 = 0$, and gives zero mean particle current but nonzero energy current. The second one is that when we apply equal bias, i.e., $\mu_1\beta_1 = \mu_2\beta_2$, the nonzero particle current signatures the presence of a nonzero pairing potential.

The third case is the Majorana case $\Delta = t$, $\mu = 0$. Two Majorana zero modes will emerge and localize at the ends of the Kitaev chain. The NT and CAR are completely suppressed, that is, $\mathcal{T}_{\rm NT} = \mathcal{T}_{\rm CAR} = 0$. The FR decouples

$$\frac{P(\Delta N_1)}{P(-\Delta N_1)} = e^{\Delta N_1 \mu_1 \beta_1}, \quad \frac{P(\Delta N_2)}{P(-\Delta N_2)} = e^{\Delta N_2 \mu_2 \beta_2}. \tag{14}$$

In this case, there is no energy transport, since LAR effectively transports two electrons with opposite energy to the chain. The net exchange of particle number is two, while the net exchange of energy is zero. The expression of transmission coefficient of LAR $\mathcal{T}_{{\rm LAR},\alpha}$ in the third case is independent of the site number [42]. It can be proved that the Kitaev chain in the third case is equivalent to a three-level system. The above discussion of the MZM case applies when the localized MZMs do not overlap, i.e., the LAR dominates the transport of the system. At the "sweet point" $\mu = 0, t = \Delta$, the lowest two Majorana modes are exactly degenerate with zero energy. The wave functions of these two MZMs are perfectly localized at two ends of the chain. If we increase $|\mu|$ and the system deviates from the "sweet point," then the wave functions will extend from two ends to the bulk. As long as the penetration length is less than $N/2$, i.e., the wave function of the two sides do not overlap, the gap between the two Majorana modes are approximately zero. In this case, we say that the system is in a topological superconducting (TSC) phase. In the thermodynamic limit $N \to \infty$, the overlap occurs when $|\mu| \geqslant 2t$. For a finite chain, the chemical potential $|\mu|$ at which the two wave functions begin to overlap can be determined by requiring the system has a zero energy solution and is found to be $|\mu| = 2N/(N+1)$ [43,44]. For a short chain, the TSC phase will shrink in the phase diagram due to the finite-size effect (see Fig. 2). In summary, all three subprocesses contribute to the particle current, but only NT and CAR contribute to the energy flow.

IV. LINEAR RESPONSE IN KITAEV CHAIN

The FCS encodes all the information about the transport process. All the cumulants can be generated from the cumulant generating function (CGF) which is defined as

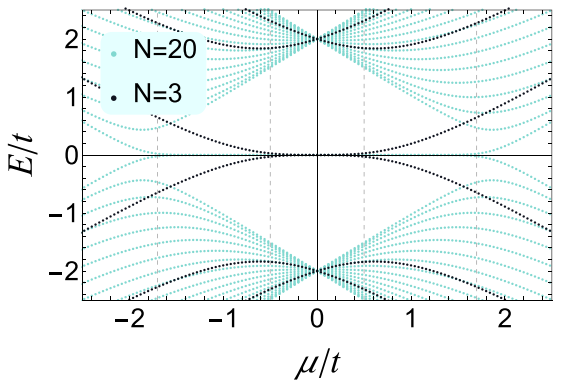

FIG. 2. The energy spectrum of a Kitaev chain with open boundaries. Dark points are for 3 sites; light points are for 20 sites. The regime for TSC phase is reduced to about $|\mu/t| < 0.5$ for a 3-site chain from about $|\mu/t| < 1.7$ for 20-site system; both are denoted as dotted vertical lines. For 20 sites, the gap opens at $|\mu/t| \sim 1.7$, while for 3 sites, the gap opens at $|\mu/t| \sim 0.5$. The phase boundary of a Kitaev chain in the thermodynamic limit is $|\mu/t| = 2$. The shrink of the TSC phase is a manifestation of the finite-size effect.

$$\mathcal{F}(\boldsymbol{\lambda}, \boldsymbol{A}) \equiv \lim_{\tau\to\infty} \frac{1}{\tau} \ln Z(\boldsymbol{\lambda}, \boldsymbol{A}), \tag{15}$$

where we update the definition of counting fields $\boldsymbol{\lambda} = \{\lambda_1, \lambda_2, \lambda_3\} \equiv \{\xi_1, \xi_2, \eta_-\}$. The affinities are denoted as $\boldsymbol{A} = \{\boldsymbol{A}_N, A_E\}$. By taking successive derivatives of the CGF with respect to the counting fields and setting them to zero, we obtain expressions for various cumulants. For instance, the mean current (the first cumulant) and the current noise (the second cumulant) are given by

$$J_j(\boldsymbol{A}) \equiv \left.\frac{\partial \mathcal{F}(\boldsymbol{\lambda}, \boldsymbol{A})}{\partial(i\lambda_j)}\right|_{\boldsymbol{\lambda}=0}, \tag{16}$$

$$D_{jk}(\boldsymbol{A}) \equiv \left.\frac{\partial^2 \mathcal{F}(\boldsymbol{\lambda}, \boldsymbol{A})}{\partial(i\lambda_j)\partial(i\lambda_k)}\right|_{\boldsymbol{\lambda}=0}. \tag{17}$$

The CGF inherits the symmetry in the MGF [Eq. (10)]

$$\mathcal{F}(\boldsymbol{\lambda}, \boldsymbol{A}) = \mathcal{F}(-\boldsymbol{\lambda} + i\boldsymbol{A}, \boldsymbol{A}), \tag{18}$$

which implies a universal relation between the cumulants and response coefficients [16,18,19]. The first-order relation is nothing but the Onsager reciprocal relation and FDR. In Appendix A, we demonstrate the response relation up to the second order by explicit expression of the response coefficients.

In this section, we focus on the linear response regime. The linear response of the Kitaev chain, has been extensively studied [40,44–52]. The most important results are the quantized zero bias peak in the local electrical conductance when the Kitaev chain is in the TSC phase, and the half-quantized peak in the thermal conductance when the Kitaev chan undergoes topological phase transition [51,53–55].

From Eq. (16), we obtain the expression of the particle current J_1^N from the left reservoir and J_2^N from the right reservoir,

as well as the energy current J_1^E from the left reservoir

$$J_1^N = \int \frac{d\omega}{2\pi}[\mathbb{T}_{\rm NT}(p_{e\to e} - p_{e\leftarrow e}) + \mathbb{T}_{\rm CAR}(p_{e\to h} - p_{e\leftarrow h}) + \mathbb{T}_{{\rm LAR},1}(n_{1e}\bar{n}_{1h} - \bar{n}_{1e}n_{1h})], \tag{19}$$

$$J_2^N = \int \frac{d\omega}{2\pi}[\mathbb{T}_{\rm NT}(p_{e\leftarrow e} - p_{e\to e}) + \mathbb{T}_{\rm CAR}(p_{e\to h} - p_{e\leftarrow h}) + \mathbb{T}_{{\rm LAR},2}(n_{2e}\bar{n}_{2h} - \bar{n}_{2e}n_{2h})], \tag{20}$$

$$J_1^E = \int \frac{d\omega}{2\pi}\omega[\mathbb{T}_{\rm NT}(p_{e\to e} - p_{e\leftarrow e}) + \mathbb{T}_{\rm CAR}(p_{e\to h} - p_{e\leftarrow h})], \tag{21}$$

where $p_{e\to e} = n_{1e}\bar{n}_{2e}$, $p_{e\leftarrow e} = \bar{n}_{1e}n_{2e}$, $p_{e\to h} = n_{1e}\bar{n}_{2h}$, and $p_{e\leftarrow h} = \bar{n}_{1e}n_{2h}$. The transmission coefficients are given by

$$\mathbb{T}_{\rm NT} = p_{\rm NT}\mathcal{T}_{\rm NT}, \quad \mathbb{T}_{\rm CAR} = p_{\rm CAR}\mathcal{T}_{\rm CAR}, \quad \mathbb{T}_{{\rm LAR},\alpha} = p_{\rm LAR}\mathcal{T}_{{\rm LAR},\alpha}.$$

The energy current of the right reservoir J_2^E is equal to the opposite of J_1^E, and the supercurrent J_S^N is equal to the opposite of $J_1^N + J_2^N$. Three independent currents are consistent with three affinities. As mentioned before, the energy current is carried by the particles participating in the NT and the CAR processes, while all the three transport processes contribute to the particle flow. We obtain the linear response coefficients $L_{j,k}$ relevant to J_1^N as

$$L_{1,1} = \int \frac{d\omega}{2\pi}[\mathbb{T}_{\rm NT}(\omega) + \mathbb{T}_{\rm CAR}(\omega) + 2\mathbb{T}_{{\rm LAR},1}(\omega)]n_{1e}\bar{n}_{1e}, \tag{22}$$

$$L_{1,2} = \int \frac{d\omega}{2\pi}[-\mathbb{T}_{\rm NT}(\omega)n_{2e}\bar{n}_{2e} + \mathbb{T}_{\rm CAR}(\omega)n_{2h}\bar{n}_{2h}], \tag{23}$$

$$L_{1,E} = \int \frac{d\omega}{2\pi}\omega[\mathbb{T}_{\rm NT}(\omega) + \mathbb{T}_{\rm CAR}(\omega) + 2\mathbb{T}_{{\rm LAR},1}(\omega)]n_{1e}\bar{n}_{1e}. \tag{24}$$

The linear response coefficients $L_{j,k}$ relevant to J_2^N are

$$L_{2,1} = \int \frac{d\omega}{2\pi}[-\mathbb{T}_{\rm NT}(\omega) + \mathbb{T}_{\rm CAR}(\omega)]n_{1e}\bar{n}_{1e}, \tag{25}$$

$$L_{2,2} = \int \frac{d\omega}{2\pi}[\mathbb{T}_{\rm NT}(\omega) + \mathbb{T}_{\rm CAR}(-\omega) + 2\mathbb{T}_{{\rm LAR},2}(\omega)]n_{2e}\bar{n}_{2e}, \tag{26}$$

$$L_{2,E} = \int \frac{d\omega}{2\pi}\omega[-\mathbb{T}_{\rm NT}(\omega) + \mathbb{T}_{\rm CAR}(\omega)]n_{1e}\bar{n}_{1e}. \tag{27}$$

The linear response coefficients $L_{j,k}$ relevant to J_1^E are

$$L_{E,1} = \int \frac{d\omega}{2\pi}\omega[\mathbb{T}_{\rm NT}(\omega) + \mathbb{T}_{\rm CAR}(\omega)]n_{1e}\bar{n}_{1e}, \tag{28}$$

$$L_{E,2} = \int \frac{d\omega}{2\pi}\omega[-\mathbb{T}_{\rm NT}(\omega)n_{2e}\bar{n}_{2e} + \mathbb{T}_{\rm CAR}(\omega)n_{2h}\bar{n}_{2h}], \tag{29}$$

$$L_{E,E} = \int \frac{d\omega}{2\pi}\omega^2[\mathbb{T}_{\rm NT}(\omega) + \mathbb{T}_{\rm CAR}(\omega)]n_{1e}\bar{n}_{1e}. \tag{30}$$

From Eqs. (24) and (28), it seems that Onsager reciprocal relation is apparently violated due to the presence of LAR. But actually, we have $\mathbb{T}_{{\rm LAR},1}(\omega) = \mathbb{T}_{{\rm LAR},1}(-\omega)$ as a consequence of the particle-hole symmetry, so the term containing $\mathbb{T}_{{\rm LAR},1}$ in Eq. (24) is an odd function of ω at zero affinity and vanishes after the integration. Hence, the Onsager reciprocal relation remains valid in the Kitaev chain.

In experiment, the more familiar linear response coefficients are the electrical conductance G, thermal conductance K, and Seebeck coefficient S. The effective Hamiltonian Eq. (1) suggests a two-terminal setup, but the presence of three independent currents (and three affinities) indicates that this model is actually a three-terminal system. The coupling between the nanowire and the third SC terminal is encoded in the gap Δ. A closely related system is the two Majorana modes which serves as a low-energy effective model of the Kitaev chain. We give the expression of currents and a detailed discussion of two MZMs coupled to two reservoirs in the framework of three-terminal system in Appendix B. There are already many discussions of the three-terminal system [34,35,56–58]. Most of the work focuses on the electrical conductance matrix G_{ij} and thermal conductance K in the zero temperature limit. In the following, we give a finite-temperature analysis.

In a three-terminal system, we write the relation between the currents and affinities in the linear response regime as

$$\begin{pmatrix} J_1^N \\ J_2^N \\ J_1^Q \end{pmatrix} = \begin{pmatrix} L_{1,1} & L_{1,2} & L_{1,E} \\ L_{2,1} & L_{2,2} & L_{2,E} \\ L_{E,1} & L_{E,2} & L_{E,E} \end{pmatrix} \begin{pmatrix} \delta\mu_1/T \\ \delta\mu_2/T \\ \delta T/T^2 \end{pmatrix}, \tag{31}$$

where we take the temperature of the right reservoir as the reference temperature $T = T_2$ and $\delta T = T_1 - T_2$. The chemical potential of the grounded SC $\mu_{\rm SC} = 0$ is taken as the reference of chemical potential and $\delta\mu_\alpha \equiv \mu_\alpha - \mu_{\rm SC} = \mu_\alpha$. The heat current from the left reservoir is defined as $J_1^Q \equiv J_1^E - \mu_1 J_1^N$ as a result of thermodynamical laws [59]. Following Ref. [60], the electrical conductance is obtained under the isothermal condition, i.e.,

$$G_{ij} = \left(\frac{e^2 J_i^N}{\delta\mu_j}\right)_{\substack{\delta T=0 \\ \delta\mu_k=0\ k\neq i}} = \frac{e^2}{T}\begin{pmatrix} L_{1,1} & L_{1,2} \\ L_{2,1} & L_{2,2} \end{pmatrix}. \tag{32}$$

Here, G_{11} and G_{22} are the local electrical conductances and $G_{12}(= G_{21})$ is the nonlocal electrical conductance. The Seebeck coefficients are obtained as the ratio of the voltage difference and the temperature difference when there are no electrical currents, i.e.,

$$S_{jE} = -\left(\frac{\delta\mu_j}{e\delta T}\right)_{J_k^N=0\ \forall k}.$$

We find

$$S_{1E} = \frac{1}{eT}\frac{L_{1,E}L_{2,2} - L_{1,2}L_{2,E}}{L_{1,1}L_{2,2} - L_{1,2}L_{2,1}}, \quad S_{2E} = \frac{1}{eT}\frac{L_{1,1}L_{2,E} - L_{1,E}L_{1,2}}{L_{1,1}L_{2,2} - L_{1,2}L_{2,1}}. \tag{33}$$

The Peltier coefficient is related to Seebeck coefficient by $\Pi_{Ej} = TS_{jE}$. The thermal conductance is defined as the ratio of heat current and temperature difference when the particle current is zero, i.e.,

$$K = \left(\frac{J_1^Q}{\delta T}\right)_{J_k^N=0\ \forall k} = \frac{1}{T^2}(L_{E,E} - TL_{E,1}S_{1E} - TL_{E,2}S_{2E}). \tag{34}$$

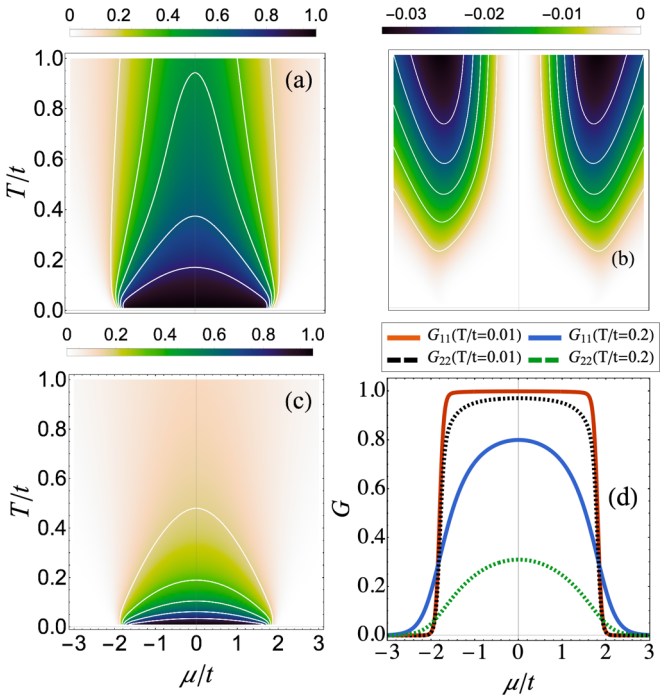

FIG. 3. The electrical conductance G_{11}, G_{12}, and G_{22} in units of $2e^2/h$ for a 20-site Kitaev chain. The parameters are set to be $t = \Delta = 1$, and we adopt asymmetric coupling strengths $\Gamma_1/t = 0.5, \Gamma_2/t = 0.1$. (a–c) are for G_{11}, G_{12}, and G_{22}, respectively. (d) Cross sections of electrical conductances for a low temperature $T/t = 0.01$ and a high temperature $T/t = 0.2$. The local conductances G_{11} and G_{22} are quantized at low temperature when $|\mu| < t$, which indicates the current component of LAR dominates the transport process.

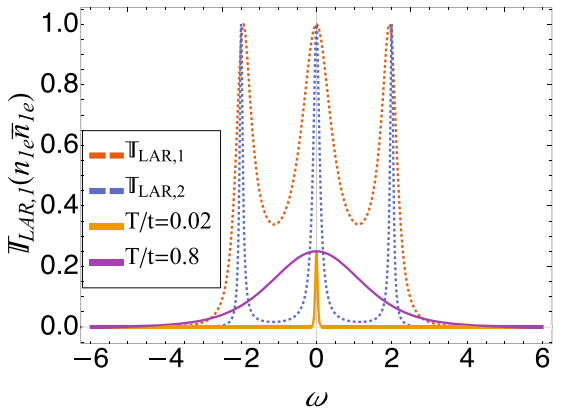

FIG. 4. The transmission functions $\mathbb{T}_{\mathrm{LAR},\alpha}$ (dashed line) and Fermi-Dirac factor $n_{1e}\bar{n}_{1e}$ (solid line) at $T/t = 0.02, 0.8$. The parameters are $\mu = 0$, $t = \Delta = 1$, $\Gamma_1 = 0.5$, and $\Gamma_2 = 0.1$. At low temperature, due to the small number of excitation, the factor $n_{1e}\bar{n}_{1e}$ are concentrated around $\omega = 0$, where the two transmissions have identical values. Consequently, the local conductances G_{11} and G_{22} are relatively close to each other. At high temperature, as the thermal excitation distribution broadens, the discrepancy between the transmission functions leads to significant differences in the local conductances G_{11} and G_{22}.

From Eqs. (32)–(34), we recognize that the electrical conductance between the left reservoir and the chain is still given by $G_{11} = L_{1,1}/T$, which is identical to the two-terminal case. Nevertheless, the expressions for Seebeck coefficients S_{jE} and thermal conductance K are different from the two-terminal case [61].

In Refs. [44,62], the local electrical conductance for a symmetric bias configuration $\mu_1 = -\mu_2 = \delta\mu/2$ when the Kitaev chain is in the TSC phase, is found to be half-quantized at e^2/h instead of the expected $2e^2/h$. This discrepancy arises from the use of different definitions for the local conductance. While those references define it as $\delta I/\delta\mu$, a more reasonable definition is $\delta I/\delta\mu_1 = 2\delta I/\delta\mu$ from Eq. (32).

As mentioned in Sec. II, we measure all energy in the unity of t. The superconductor gap of a typical InSb-Al nanowire devices is of order $\sim$100 μeV $\approx$ 1.6 K, and the working temperature is around 0.02 K. We choose our parameters as $\Delta/t = 1$ and vary the temperature T/t from 0.01 to 1 following the experiment. Under this choice, $\mu = 0$ corresponds to perfect MZM case and only LARs are present. We plot the electrical conductances G for different μ at finite temperature for a 20-site model in Fig. 3. We adopt the asymmetric effective coupling strengths $\Gamma_1/t = 0.5$, $\Gamma_2/t = 0.1$ [63]. We find the local electrical conductance [Figs. 3(a) and (c)] is nearly unity at low T in the region $|\mu| < 1.7t$. It is consistent with the spectrum of a 20-site model in Fig. 2 which shows that the nanowire hosts Majorana modes at two ends of the wire when $|\mu| < 1.7t$. In contrast, the nonlocal electrical conductance [Fig. 3(b)] is small at low temperature and is nonzero near the gap-opening region. The low-temperature feature of the electrical conductances of the left and right reservoirs is quite similar even though the coupling strengths are asymmetric. As the temperature increases, high-energy modes begin to get involved, and the asymmetry in the coupling strengths affect the conductance dramatically. For example, at $T = 0.2$, the electrical conductance of the left reservoir G_{11} is nearly three times of the right one G_{22} [see Fig. 3(d)]. This distinction becomes evident when we examine the region $\mu \ll t$ in which the transport is primarily governed by the LAR. The transmission functions of the left LAR and the right LAR at the sweet point $\mu = 0$, $\Delta = t = 1$ are [25]

$$\mathbb{T}^{\mathrm{sp}}_{\mathrm{LAR},\alpha}(\omega) = \frac{16\Gamma_\alpha^2}{\Gamma_\alpha^4\omega^2 + \omega^2(\omega^2-4)^2 + 2\Gamma_\alpha^2(\omega^4 - 4\omega^2 + 8)}.$$

At low temperature, the small number of excitations leads to a concentration of the factor $n_{1e}\bar{n}_{1h}$ near $\omega = 0$, where the two transmission functions exhibit similar values, resulting in an almost equal local electrical conductance. However, at higher temperature, the broader excitation distribution spreads over a wide frequency range, causing the discrepancy between the transmission functions to significantly affect the conductance G_{11} and G_{22} (see Fig. 4). As the chemical potential μ increases, the LAR is suppressed and the normal transport becomes dominant, causing the two conductances G_{11} and G_{22} to converge.

In Fig. 5, we show the thermal conductance K/T as a function of T/t and μ/t. We see that the K/T is nearly zero in the region $|\mu| < 1.7t$ and increases dramatically in the vicinity of the gap opening point $|\mu|/t \sim 1.7$, which is different from the behavior of local electrical conductance.

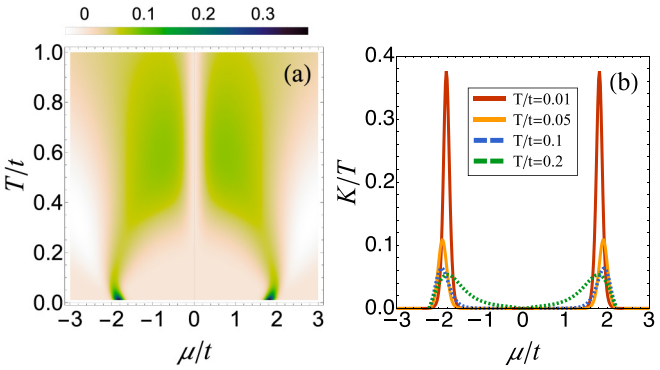

FIG. 5. Thermal conductance in units of $\pi^2 k_B^2/3h$ of a 20-site Kitaev chain. The parameters are $t = \Delta = 1$, and we adopt asymmetric coupling $\Gamma_1 = 0.5$, $\Gamma_1 = 0.1$. (a) The temperature and chemical potential dependence of K/T. (b). Cross sections of thermal conductance at various T.

The zero value of thermal conductance is due to the fact that LAR does not transfer energy. It can also be seen in Fig. 5(b). When $\mu = 0$, the system is in the exactly solvable case. Two Majorana modes are perfectly localized at two ends of the chain. NT and CAR vanish and only LAR is present. There is no energy transport, so the thermal conductance is always zero regardless of the temperature. Another interesting feature is that the peak at low temperature $T/t = 0.01$ is close to half of a thermal conductance quantum $(1/2)\pi k_B^2/3h$. Similar feature is also seen in the two Majorana modes system (see Appendix B). Previous works show the peak is exactly half quantized at the phase transition point in the long chain limit [53], and numerical studies show it is also the case in the finite chain case [51,52]. We prove that the half quantization is exact in the zero temperature limit for a finite Kitaev chain and the two Majorana modes system in Appendices A and B.

V. SUMMARY

In this article, we obtain a general form of the MGF of energy and particle transport in an 1D open Kitaev chain at finite temperature. The explicit expression of the MGF allows us to extract the fluctuation relations in a straightforward manner. The energy current is carried by the particles involved in the NT process and the CAR process, while the particle current is also carried by the LAR process in addition to the above two processes. We find that the joint distribution of particle and energy currents satisfies different fluctuation relations in different regions of the parameter space as a result of U(1) symmetry breaking and energy conservation. Moreover, we study the linear response properties of the Kitaev chain in the framework of three-terminal system. The electrical conductance is quantized in the TSC phase when the Kitaev chain hosts two Majorana modes at two ends as expected. The thermal conductance, however, is half quantized at the phase transition point.

In addition to its significance in the field of Majorana physics, the Kitaev chain could serve as a thermal machine outside the TSC phase and it offers a promising platform for exploring thermodynamics of three-terminal system, in parallel to other three-terminal systems, such as the phonon-thermoelectric systems [60,64–71], or the Cooper-pair splitter [72–75]. Future investigations in this direction could delve into the analysis of work power and efficiency across different phases, as well as exploring the impact of finite size effects, with the help of our exact expression of MGF.

ACKNOWLEDGMENTS

We thank R. Sánchez for pointing out relevant works on three-terminal systems and Cooper-pair splitters. We acknowledge support from the National Natural Science Foundation of China under Grants No. 11775001, No. 11825501, and No. 12147162.

APPENDIX A: EXPRESSION OF THE FACTORS IN THE MGF

In this Appendix, we give the exact expression of factors in the MGF (9). First we calculate the nonequilibrium Green's function (GF) of the Kitaev chain. We choose the site-ordered particle-hole basis

$$\hat{\Psi} = (\hat{d}_1^\dagger \quad \dots \quad d_N \quad \hat{d}_N^\dagger)^T.$$

In this basis, the Hamiltonian of the Kitaev chain can be written as

$$\hat{H}_K = \tfrac{1}{2}\hat{\Psi}^T \mathcal{H} \hat{\Psi},$$

where $\mathcal{H}$ is an antisymmetric block tridiagonal matrix

$$\mathcal{H} = \begin{pmatrix} i\sigma_y\mu & \mathcal{D} & 0 & \dots & \dots & 0 \\ \mathcal{D}^T & i\sigma_y\mu & \mathcal{D} & 0 & \dots & 0 \\ 0 & \mathcal{D}^T & \ddots & \ddots & \ddots & \vdots \\ \vdots & \ddots & \ddots & \ddots & \mathcal{D} & 0 \\ 0 & \dots & 0 & \mathcal{D}^T & i\sigma_y\mu & \mathcal{D} \\ 0 & \dots & \dots & 0 & \mathcal{D}^T & i\sigma_y\mu \end{pmatrix},$$

with

$$\mathcal{D} \equiv i\sigma_y^T t + \Delta\sigma_z = \begin{pmatrix} \Delta & t \\ -t & -\Delta \end{pmatrix}$$

and σ_j $(j = x, y, z)$ the Pauli matrix. The free GF is given by

$$\mathcal{G} = (i\partial_t - \mathcal{H} - \Sigma)^{-1}, \tag{A1}$$

where Σ is the self-energy of the reservoirs

$$\Sigma = \begin{pmatrix} \Sigma_1 & 0 & \dots & 0 \\ 0 & 0 & \dots & 0 \\ \vdots & \ddots & \ddots & \vdots \\ \vdots & \ddots & \ddots & 0 \\ 0 & \dots & 0 & \Sigma_N \end{pmatrix},$$

with

$$\Sigma_\alpha = \begin{pmatrix} \Sigma_{\alpha e} & \\ & \Sigma_{\alpha h} \end{pmatrix}.$$

Under the wide-band approximation, the self-energy of reservoir α is given by

$$\Sigma_{\alpha e} = -i\Gamma_\alpha \begin{pmatrix} 1 & 2(1-n_{\alpha e}) \\ 0 & -1 \end{pmatrix},$$
$$\Sigma_{\alpha h} = -i\Gamma_\alpha \begin{pmatrix} 1 & 2(1-n_{\alpha h}) \\ 0 & -1 \end{pmatrix}.$$

Here, the subscript (e, h) indicates the self-energy of electrons or holes. The free GF can be divided into $N \times N$ blocks. Each block is a 4×4 matrix

$$[\mathcal{G}]_{ij} = \begin{pmatrix} [\mathcal{G}]_{ij}^{eh} & [\mathcal{G}]_{ij}^{ee} \\ [\mathcal{G}]_{ij}^{hh} & [\mathcal{G}]_{ij}^{he} \end{pmatrix},$$

and its element $[\mathcal{G}]_{ij}^{\alpha\beta}$ $(\alpha, \beta = e, h)$ enjoys a so-called causality structure

$$[\mathcal{G}]_{ij}^{\alpha\beta} = \begin{pmatrix} [\mathcal{G}^K]_{ij}^{\alpha\beta} & [\mathcal{G}^R]_{ij}^{\alpha\beta} \\ [\mathcal{G}^A]_{ij}^{\alpha\beta} & 0 \end{pmatrix},$$

with $\mathcal{G}^R$, $\mathcal{G}^A$, $\mathcal{G}^K$ the retarded, advanced, and Keldysh GFs, respectively. Now we introduce the scattering matrix which is related to GF by Fisher-Lee formula [76]

$$\mathcal{S} = \mathrm{I} - i\sqrt{i\Sigma}\mathcal{G}^R\sqrt{i\Sigma}, \quad \mathcal{S}^\dagger = \mathrm{I} + i\sqrt{i\Sigma}\mathcal{G}^A\sqrt{i\Sigma}.$$

The scattering matrix is unitary

$$\mathcal{S}\mathcal{S}^\dagger = \mathcal{S}^\dagger\mathcal{S} = \mathrm{I}$$

and can be written as

$$\mathcal{S} = \begin{pmatrix} \boldsymbol{r}_{11} & \boldsymbol{r}_{12} & \dots & \boldsymbol{r}_{1N} \\ \boldsymbol{r}_{21} & \boldsymbol{r}_{22} & \dots & \vdots \\ \vdots & \ddots & \ddots & \vdots \\ \boldsymbol{r}_{N1} & \dots & \dots & \boldsymbol{r}_{NN} \end{pmatrix},$$

where the reflection matrix $\boldsymbol{r}_{jk}$ has a 2×2 block structure in the particle-hole space

$$\boldsymbol{r}_{jk} = \begin{pmatrix} r_{jk}^{eh} & r_{jk}^{ee} \\ r_{jk}^{hh} & r_{jk}^{he} \end{pmatrix}.$$

Here r_{jj}^{eh}, r_{jk}^{ee}, and r_{jk}^{eh} are the usual amplitude of the LAR at site j, the amplitude of the NT from site j to site k, and the amplitude of the CAR from site j to site k, respectively.

With the help of the scattering matrix, we find that

$$\mathbb{T}_{\mathrm{NT}} = p_{\mathrm{NT}}\mathcal{T}_{\mathrm{NT}} = \left|r_{1N}^{ee}\right|^2 = 4\Gamma_1\Gamma_2\left[\mathcal{G}_{1N}^R\right]^{ee}\left[\mathcal{G}_{N1}^A\right]^{ee},$$
$$\mathbb{T}_{\mathrm{CAR},e} = p_{\mathrm{CAR}}\mathcal{T}_{\mathrm{CAR}} = \left|r_{1N}^{eh}\right|^2 = 4\Gamma_1\Gamma_2\left[\mathcal{G}_{1N}^R\right]^{eh}\left[\mathcal{G}_{N1}^A\right]^{he},$$
$$\mathbb{T}_{\mathrm{LAR},1} = p_{\mathrm{LAR}}\mathcal{T}_{\mathrm{LAR},1} = \left|r_{11}^{eh}\right|^2 = 4\Gamma_1^2\left[\mathcal{G}_{11}^R\right]^{he}\left[\mathcal{G}_{11}^A\right]^{eh},$$
$$\mathbb{T}_{\mathrm{LAR},2} = p_{\mathrm{LAR}}\mathcal{T}_{\mathrm{LAR},2} = \left|r_{NN}^{eh}\right|^2 = 4\Gamma_2^2\left[\mathcal{G}_{NN}^R\right]^{he}\left[\mathcal{G}_{NN}^A\right]^{eh},$$

and

$$p_{\mathrm{NT}}\mathcal{T}_{\mathrm{NT}}\bar{\mathcal{T}}_{\mathrm{NT}} = \mathbb{T}_{\mathrm{NT}} - \det[\mathcal{S}_{ee}^\dagger\mathcal{S}_{ee}],$$
$$p_{\mathrm{CAR}}\mathcal{T}_{\mathrm{CAR}}\bar{\mathcal{T}}_{\mathrm{CAR}} = \mathbb{T}_{\mathrm{CAR}} - \det[\mathcal{S}_{eh}^\dagger\mathcal{S}_{eh}],$$
$$p_{\mathrm{LAR}}\mathcal{T}_{\mathrm{LAR},1}\mathcal{T}_{\mathrm{LAR},2} = \mathbb{T}_{\mathrm{LAR},1} - \det[\mathcal{S}_L^\dagger\mathcal{S}_L],$$

where

$$\mathcal{S}_{ee} = \begin{bmatrix} r_{11}^{eh} & r_{1N}^{ee} \\ r_{11}^{hh} & r_{1N}^{he} \end{bmatrix}, \mathcal{S}_{eh} = \begin{bmatrix} r_{11}^{eh} & r_{1N}^{eh} \\ r_{11}^{hh} & r_{1N}^{he} \end{bmatrix}, \mathcal{S}_L = \begin{bmatrix} r_{11}^{eh} & r_{1N}^{ee} \\ r_{1N}^{eh} & r_{11}^{ee} \end{bmatrix}.$$

We only need to find the expression of the retarded GF since $\mathcal{G}^A$ is the complex conjugate of $\mathcal{G}^R$. The block tridiagonal structure of the GF allows us to obtain an exact expression of the retarded GF. The inverse of the retarded GF in frequency space can be read out from the GF (A1)

$$[\mathcal{G}^R]^{-1}(\omega) = \begin{pmatrix} \boldsymbol{D}_1 & \boldsymbol{B} & 0 & \dots & \dots & 0 \\ \boldsymbol{B}^T & \boldsymbol{D} & \boldsymbol{B} & 0 & \dots & 0 \\ 0 & \boldsymbol{B}^T & \ddots & \ddots & \ddots & \vdots \\ \vdots & \ddots & \ddots & \ddots & & 0 \\ 0 & \dots & 0 & \boldsymbol{B}^T & \boldsymbol{D} & \boldsymbol{B} \\ 0 & \dots & \dots & 0 & \boldsymbol{B}^T & \boldsymbol{D}_N \end{pmatrix},$$

which is a $2N \times 2N$ block tridiagonal matrix with diagonal block elements

$$\boldsymbol{D}_1 = \begin{bmatrix} \omega + \mu + i\Gamma_1 & \\ & \omega - \mu + i\Gamma_1 \end{bmatrix},$$
$$\boldsymbol{D}_N = \begin{bmatrix} \omega + \mu + i\Gamma_2 & \\ & \omega - \mu + i\Gamma_2 \end{bmatrix},$$
$$\boldsymbol{D}_n = \begin{bmatrix} \omega + \mu & \\ & \omega - \mu \end{bmatrix}, \quad \text{for} \quad 1 < n < N,$$

and the subdiagonal block element

$$\boldsymbol{B} = \begin{bmatrix} -t & -\Delta \\ \Delta & t \end{bmatrix}.$$

Now we can use the formula of inverse of block tridiagonal matrices in Refs. [77–80]. We introduce two matrix sequences $\{\mathcal{X}_n\}$ and $\{\mathcal{Y}_n\}$, which are obtained recursively

$$\mathcal{X}_n = \begin{cases} 0 & \text{if } n = N, \\ \boldsymbol{B}[\boldsymbol{D}_{n+1} - \boldsymbol{X}_{n+1}]^{-1}\boldsymbol{B}^T & \text{if } 1 \leqslant n < N, \end{cases} \tag{A2}$$
$$\mathcal{Y}_n = \begin{cases} 0 & \text{if } n = 1, \\ \boldsymbol{B}^T[\boldsymbol{D}_{n-1} - \boldsymbol{Y}_{n-1}]^{-1}\boldsymbol{B} & \text{if } 1 \leqslant n < N. \end{cases} \tag{A3}$$

Then the diagonal block of $\mathcal{G}^R$ is given by

$$\mathcal{G}_{n,n}^R(\omega) = [\boldsymbol{B} - \mathcal{X}_n - \mathcal{Y}_n]^{-1}, \tag{A4}$$

and the off-diagonal blocks are

$$\mathcal{G}_{m,n}^R = \begin{cases} -[\boldsymbol{D}_m - \mathcal{X}_m]^{-1}\boldsymbol{B}_{m-1}^T\mathcal{G}_{m-1,n}^R & \text{if } m > n, \\ -[\boldsymbol{D}_m - \mathcal{Y}_m]^{-1}\boldsymbol{B}_{m-1}\mathcal{G}_{m+1,n}^R & \text{if } m < n. \end{cases} \tag{A5}$$

Even though the computations scale linearly with N, each step in the recurrence can be expensive. The near block

Toeplitz form of $[\mathcal{G}^R]^{-1}$ allows us to obtain a compacted form. We introduce the *matrix Möbius transformation* which is defined as

$$\boldsymbol{T}\circ z \equiv (\boldsymbol{a}\cdot z+\boldsymbol{b})(\boldsymbol{c}\cdot z+\boldsymbol{d})^{-1}, \tag{A6}$$

where z is a 2×2 matrix and $\boldsymbol{T}$ a 4×4 block matrix with block elements

$$\boldsymbol{T}=\begin{bmatrix}\boldsymbol{a} & \boldsymbol{b}\\ \boldsymbol{c} & \boldsymbol{d}\end{bmatrix}.$$

The dot operation $\cdot$ in the right-hand side of Eq. (A6) is the usual matrix product. The Möbius transformation is associative, namely,

$$\boldsymbol{S}\circ(\boldsymbol{T}\circ z)=(\boldsymbol{S}\cdot\boldsymbol{T})\circ z$$

for two 4×4 block matrix $\boldsymbol{S}$ and $\boldsymbol{T}$. Hence, we rewrite the recurrence relation (A2) of $\{\mathcal{X}_n\}$ $(1<n<N)$ except the boundary terms as

$$\begin{aligned}\mathcal{X}_n &= \boldsymbol{B}[(\boldsymbol{B}^T)^{-1}\boldsymbol{D}_{n+1}-(\boldsymbol{B}^T)^{-1}\mathcal{X}_{n+1}]\\ &=\begin{bmatrix}0 & \boldsymbol{B}\\ -(\boldsymbol{B}^T)^{-1} & (\boldsymbol{B}^T)^{-1}\boldsymbol{D}\end{bmatrix}\circ\mathcal{X}_{n+1}\\ &=\begin{bmatrix}0 & \boldsymbol{B}\\ -(\boldsymbol{B}^T)^{-1} & (\boldsymbol{B}^T)^{-1}\boldsymbol{D}\end{bmatrix}^{N-1-n}\circ\mathcal{X}_{N-1}.\end{aligned} \tag{A7}$$

Similarly, the recurrence relation (A3) of $\{\mathcal{Y}_n\}$ $(1<n<N)$ except the boundary terms is rewritten as

$$\mathcal{Y}_n=\begin{bmatrix}0 & \boldsymbol{B}^T\\ -\boldsymbol{B}^{-1} & \boldsymbol{B}^{-1}\boldsymbol{D}\end{bmatrix}^{n-2}\circ\mathcal{Y}_2. \tag{A8}$$

The matrix elements of $\mathcal{G}^R(\omega)$ is evaluated efficiently by using Eqs. (A4) and (A5) and Eqs. (A7) and (A8).

Equations (A7) and (A8) hold for a nonsingular $\boldsymbol{B}$. When $\boldsymbol{B}$ is singular, such as the parameter choice $t=\Delta$ in the main text, the original block tridiagonal matrix $[\mathcal{G}^R]^{-1}$ can be actually transformed to a tridiagonal matrix

$$[\tilde{\mathcal{G}}^R]^{-1}\equiv\mathcal{U}[\mathcal{G}^R]^{-1}\mathcal{U}^T$$
$$=\begin{bmatrix}\omega+i\Gamma_1 & -\mu & & \dots & 0 & \\ -\mu & \omega+i\Gamma_1 & -2t & & & \\ & -2t & \omega & -\mu & & \\ & & -\mu & \ddots & -2t & \\ & & & -2t & \omega+i\Gamma_2 & -\mu\\ & & & & -\mu & \omega+i\Gamma_2\end{bmatrix}$$

by the $2N\times 2N$ diagonal block unitary matrix

$$\mathcal{U}_{jk}=\delta_{jk}\frac{1}{\sqrt{2}}\begin{bmatrix}1 & 1\\ 1 & -1\end{bmatrix}.$$

We denote the diagonal sequences of $[\tilde{\mathcal{G}}^R]^{-1}$ as $\{d_1,d_2,\dots d_{2N}\}$, where

$$\begin{aligned}&d_1=d_2=\omega+i\Gamma_1,\quad d_{2N-1}=d_{2N}=\omega+i\Gamma_2,\\ &d_n=\omega\quad\text{for}\quad 2<n<2N-1.\end{aligned}$$

The subdiagonal sequences of $[\tilde{\mathcal{G}}^R]^{-1}$ are denoted by $\{a_2,a_3,\dots a_{2N}\}$, with

$$a_{2n}=\mu,\quad a_{2n+1}=2t,\quad\text{for}\quad n=1,2,\dots N.$$

The inverse of a tridiagonal matrix is characterized by two sequences $\{x_n\}$ and $\{y_n\}$ which are obtained recursively with the help of the sequences $\{d_n\}$ and $\{a_n\}$ [77], namely,

$$\begin{aligned}&x_{2N}=d_{2N},\\ &x_j=d_j-\frac{a_{j+1}^2}{x_{j+1}},\quad j=2N-1,\dots,1,\end{aligned}$$

and

$$\begin{aligned}&y_1=d_1,\\ &y_j=d_j-\frac{a_j^2}{y_{j-1}},\quad j=2,\dots,2N.\end{aligned}$$

The retarded GFs associated with NT, CAR, and LAR are given by

$$\begin{aligned}\left[\mathcal{G}^R_{1N}\right]^{ee}&=\frac{1}{2}\frac{a_2\dots a_{2N-1}}{y_1\dots y_{2N}}(x_{2N}+a_{2N})(1+y_1/a_2),\\ \left[\mathcal{G}^R_{1N}\right]^{eh}&=\frac{1}{2}\frac{a_2\dots a_{2N-1}}{y_1\dots y_{2N}}(x_{2N}-a_{2N})(1+y_1/a_2),\\ \left[\mathcal{G}^R_{11}\right]^{eh}&=\frac{1}{2}\frac{1}{x_1}(1-y_1/x_2),\\ \left[\mathcal{G}^R_{11}\right]^{eh}&=\frac{1}{2y_{2N}}(x_{2N}/y_{2N-1}-1).\end{aligned}$$

1. Half-quantized thermal conductance

We find numerically that the linear thermal conductance is nearly half quantized $K/T\sim\pi^2k_B^2/(6h)$ in the low-temperature regime (see Fig. 5). Now we prove that the half quantization is actually exact in the zero-temperature limit. We first rescale the parameters by the temperature, e.g., $\omega\to\omega/T$ and $\Gamma_\alpha\to\Gamma_\alpha/T$. At the zero temperature $T\to 0$, the value of the transmission coefficient $\mathbb{T}_{\rm NT}(\omega)$ can be

approximated by $\mathbb{T}_{\rm NT}(0)$ (same for $\mathbb{T}_{\rm CAR}$ and $\mathbb{T}_{\rm LAR}$). Then the thermal electrical response coefficients are all zero, for example,

$$\begin{aligned} L_{E,1} &= \int \frac{d\omega}{2\pi}\omega[\mathbb{T}_{\rm NT}(\omega)+\mathbb{T}_{\rm CAR}(\omega)]n_{1e}\bar{n}_{1e} \\ &= T^2[\mathbb{T}_{\rm NT}(0)+\mathbb{T}_{\rm CAR}(0)]\int \frac{d\omega}{2\pi}\frac{\omega}{4\cosh^2(\omega/2)} \\ &= 0. \end{aligned}$$

Notice that the thermal conductance K [Eq. (34)] can be written as

$$K = \frac{1}{T^2}\frac{\det L}{T\det G},$$

where L is the 3×3 linear response matrix in Eq. (31) and G is the linear electrical conductance matrix in Eq. (32). Since the thermal electrical response coefficients are all zero $L_{E,1} = L_{E,2} = L_{1,E} = L_{2,E} = 0$, the thermal conductance reduces to

$$\begin{aligned} K &= \frac{1}{T^2}L_{E,E} = T[\mathbb{T}_{\rm NT}(0)+\mathbb{T}_{\rm CAR}(0)]\int \frac{d\omega}{2\pi}\frac{\omega^2}{4\cosh^2(\omega/2)} \\ &= \frac{\pi}{6}[\mathbb{T}_{\rm NT}(0)+\mathbb{T}_{\rm CAR}(0)]T. \end{aligned}$$

From the expression of $\mathcal{G}^R_{1N}$, we obtain the expression of $\mathbb{T}_{\rm NT}(0)$ and $\mathbb{T}_{\rm CAR}(0)$,

$$\begin{aligned} \mathbb{T}_{\rm NT}(0) &= \mathbb{T}_{\rm CAR}(0) \\ &= \Gamma_1\Gamma_2\frac{\mu^{2N-4}\left(\Gamma_1^2+\mu^2\right)\left(\Gamma_2^2+\mu^2\right)(2t)^{2N}}{\left[\left(\Gamma_1^2+\mu^2\right)\left(\Gamma_2^2+\mu^2\right)\mu^{2N-4}+\Gamma_1\Gamma_2(2t)^{2N-2}\right]^2} \\ &\leqslant \frac{1}{4}, \end{aligned}$$

where the equality is achieved when

$$\frac{\left(\Gamma_2^2+\mu^2\right)\left(\Gamma_1^2+\mu^2\right)}{(2t)^4}\left(\frac{\mu}{2t}\right)^{2N-4} = \frac{\Gamma_1\Gamma_2}{(2t)^2}. \tag{A9}$$

Thus, the thermal conductance is bounded by the half-thermal conductance quantum

$$K/T = \frac{\pi}{6}[\mathbb{T}_{\rm NT}(0)+\mathbb{T}_{\rm CAR}(0)] \leqslant \frac{\pi}{12} = \frac{1}{2}\frac{\pi^2 k_B^2}{3h},$$

where we resort to SI unit in the last equality.

The location of the peak of K/T is determined numerically by solving Eq. (A9) or estimated as follows. We expect the solution to Eq. (A9) is around the phase transition point $\mu/2t = \pm 1$. We write $\mu/2t = 1+d\mu$, substitute it into Eq. (A9), and expand the left-hand side to the first order of $d\mu$. The solution is

$$\begin{aligned} d\mu = &\frac{\Gamma_1\Gamma_2 - \left(4t^2+\Gamma_1^2\right)\left(4t^2+\Gamma_2^2\right)}{2\left(4t^2+\Gamma_1^2+\Gamma_2^2\right)+\left(4t^2+\Gamma_1^2\right)\left(4t^2+\Gamma_2^2\right)(n-2)} \\ &+ \mathrm{O}\left(\frac{1}{n^2}\right). \end{aligned} \tag{A10}$$

We see that $d\mu \sim 1/(n-2)$ and the solution is indeed around the phase transition point $\mu/2t = \pm 1$ for $N \gg 1$. In Fig. 6(a), the linear thermal conductance K/T is indeed asymptotically converge to the half-thermal conductance quantum for the chemical potential μ solved from Eq. (A9) as temperature goes to zero. From Fig. 6(b), we verify our expectation that the solution of Eq. (A9) $\mu/2t \to 1$ as we approach the thermodynamic limit.

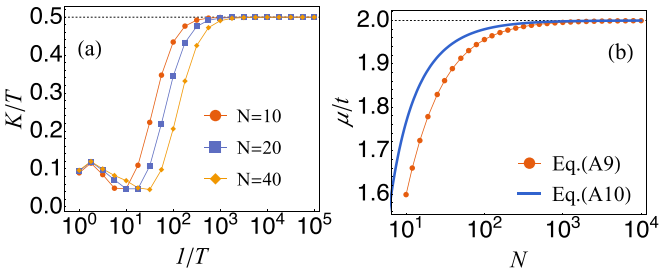

FIG. 6. (a) Linear thermal conductance K/T in units of $\pi^2 k_B^2/3h$ at the phase transition point for the Kitaev chain with site number $N = 10, 20, 40$. The parameters are $t = \Delta = 1$, and we adopt asymmetric coupling strengths $\Gamma_1 = 0.5, \Gamma_2 = 0.1$. The chemical potential $|\mu|$ is solved from Eq. (A9), and $|\mu| \approx 1.60, 1.79, 1.89$ for $N = 10, 20, 40$, respectively. (b) The chemical potential μ calculated from Eq. (A9) and Eq. (A10) when K/T is half quantized.

2. Response theory from FR

In this section, we first review the response theory which is derived from the exchange FR [16,18,19], including the well-known results in linear response theory, such as the Onsager reciprocal relation and FDR. Then we obtain the exact expression of nonlinear response coefficients of the Kitaev chain.

At equilibrium ($\mathbf{A} = \mathbf{0}$), the mean current vanishes. We notice that the mean current can be expanded in powers of the affinities close to equilibrium

$$J_j = \sum_k L_{j,k}A_k + \frac{1}{2}\sum_{k,l} M_{j,kl}A_kA_l + \ldots.$$

This expansion implies a definition of the response coefficients

$$L_{j,k} \equiv \left.\frac{\partial^2\mathcal{F}(\boldsymbol{\lambda},\boldsymbol{A})}{\partial(i\lambda_j)\partial A_k}\right|_{\substack{\boldsymbol{\lambda}=0\\ \boldsymbol{A}=0}}, \tag{A11}$$

$$M_{j,kl} \equiv \left.\frac{\partial^3\mathcal{F}(\boldsymbol{\lambda},\boldsymbol{A})}{\partial(i\lambda_j)\partial A_k\partial A_l}\right|_{\substack{\boldsymbol{\lambda}=0\\ \boldsymbol{A}=0}}, \tag{A12}$$

$$N_{i,jkl} = \left.\frac{\partial^3 J_i(\boldsymbol{A})}{\partial A_j\partial A_k\partial A_l}\right|_{\boldsymbol{A}=0}, \tag{A13}$$

$$\vdots$$

The response coefficients and the cumulants satisfy a family of universal relations, which can be derived from the exchange FR (18) [16,18,19]. The first-order response relations are nothing but the FDR

$$L_{j,k} = D_{jk}(\boldsymbol{A} = 0), \tag{A14}$$

and the Onsager reciprocal relation

$$L_{k,j} = L_{j,k},$$

where the second relation is from the symmetry of $D_{jk} = D_{kj}$. Thus, we see that the two main cornerstones of linear response theory are encoded in the exchange FR.

As for nonlinear response at equilibrium, we have similar relations [16,18,19]

$$M_{i,jk} = \left(\frac{\partial D_{ij}}{\partial A_k} + \frac{\partial D_{ik}}{\partial A_j}\right)\Big|_{\boldsymbol{A}=0}, \tag{A15}$$

$$N_{i,jkl} = \left(\frac{\partial^2 D_{ij}}{\partial A_k \partial A_l} + \frac{\partial^2 D_{ik}}{\partial A_j \partial A_l} + \frac{\partial^2 D_{il}}{\partial A_j \partial A_k} - \frac{1}{2}\frac{\partial C_{ijk}}{\partial A_l}\right)\Big|_{\boldsymbol{A}=0},$$

$$\vdots$$

In the following, we will consider response properties up to the second order.

3. Demonstration of the Response relation

In this section, we check the nonlinear response relation Eq. (A15) up to the second order with the exact expression of the MGF.

We consider the second-order response coefficients $M_{1,jk}$ $(j,k = 1,2,E)$ for example. At zero affinity, $M_{1,jk}$ are given by

$$M_{1,ij} = \int \frac{d\omega}{2\pi} p_0(1-p_0)(1-2p_0)\begin{pmatrix} \mathbb{T}_{\rm NT}+\mathbb{T}_{\rm CAR} & 0 & \omega(\mathbb{T}_{\rm NT}+\mathbb{T}_{\rm CAR}+2\mathbb{T}_{\rm LAR,1}) \\ 0 & -(\mathbb{T}_{\rm NT}+\mathbb{T}_{\rm CAR}) & 0 \\ \omega(\mathbb{T}_{\rm NT}+\mathbb{T}_{\rm CAR}+2\mathbb{T}_{\rm LAR,1}) & 0 & \omega^2(\mathbb{T}_{\rm NT}+\mathbb{T}_{\rm CAR}) \end{pmatrix}.$$

Accordingly, the derivative of noise D_{1j} are given by

$$\frac{\partial D_{1i}}{\partial A_j} = \frac{1}{2}\int \frac{d\omega}{2\pi} p_0(1-p_0)(1-2p_0)\begin{pmatrix} \mathbb{T}_{\rm NT}+\mathbb{T}_{\rm CAR} & \mathbb{T}_{\rm NT}-\mathbb{T}_{\rm CAR} & \omega(\mathbb{T}_{\rm NT}+\mathbb{T}_{\rm CAR}+4\mathbb{T}_{\rm LAR,1}) \\ -\mathbb{T}_{\rm NT}+\mathbb{T}_{\rm CAR} & -\mathbb{T}_{\rm NT}-\mathbb{T}_{\rm CAR} & \omega(-\mathbb{T}_{\rm NT}+\mathbb{T}_{\rm CAR}) \\ \omega(\mathbb{T}_{\rm NT}+\mathbb{T}_{\rm CAR}) & \omega(\mathbb{T}_{\rm NT}-\mathbb{T}_{\rm CAR}) & \omega^2(\mathbb{T}_{\rm NT}+\mathbb{T}_{\rm CAR}) \end{pmatrix}.$$

It is easy to check that the nonlinear response relation Eq. (A15) is satisfied in the Kitaev chain, namely

$$M_{i,jk} = \frac{\partial D_{ij}}{\partial A_k} + \frac{\partial D_{ik}}{\partial A_j}. \tag{A16}$$

It can be checked that higher-order response relations are also valid in the Kitaev chain.

APPENDIX B: TWO-TERMINAL MAJORANA JUNCTION

In this Appendix, we study the transport of two Majorana modes localized at two ends of a nanowire. This model has been extensively studied in the literature, since it is simple enough but still captures the main features of the Majorana physics. The Hamiltonian of the whole system is composed of three parts $\hat{H} = \hat{H}_M + \sum_{\alpha=1,2}\hat{H}_\alpha + \hat{H}'_I$, where $\hat{H}_\alpha$ is given by Eq. (3) and

$$\hat{H}_M = \frac{i}{2}\epsilon_M \hat{\gamma}_1\hat{\gamma}_2,$$
$$\hat{H}'_I = \sum_j (t_{1j,1}\hat{c}^\dagger_{1j}\hat{\gamma}_1 + t_{2j,2}\hat{c}^\dagger_{2j}\hat{\gamma}_2 + \text{H.c.}).$$

Here, ϵ_M is the energy gap of the MZMs, and $\hat{H}'_I$ describes the coupling between the reservoirs and the nearest Majorana mode $\hat{\gamma}_\alpha$. The Majorana modes satisfy the anticommutation relation $\{\hat{\gamma}_\alpha, \hat{\gamma}_{\alpha'}\} = 2\delta_{\alpha\alpha'}$, and can be combined to a Dirac fermion $\hat{d}^\dagger = (\hat{\gamma}_1 + i\hat{\gamma}_2)/2$, $\hat{d} = (\hat{\gamma}_1 - i\hat{\gamma}_2)/2$ which satisfies $\{\hat{d}, \hat{d}^\dagger\} = 1$.

We use the Keldysh functional integral and obtain the MGF of this system. The MGF takes the same form as Eq. (8) but the expressions of the components are slightly different

$$Z_{M,\rm NT}(\xi_1-\xi_2) = p_{M,\rm NT} + \mathcal{T}_{M,\rm NT}[n_{1e}\bar{n}_{2e}(e^{i(\xi_1-\xi_2)}e^{i\omega\eta_-} - 1) + \bar{n}_{1e}n_{2e}(e^{-i(\xi_1-\xi_2)}e^{-i\omega\eta_-} - 1)]$$
$$+ \bar{\mathcal{T}}_{M,\rm NT}[n_{1h}\bar{n}_{2h}(e^{-i(\xi_1-\xi_2)}e^{i\omega\eta_-} - 1) + \bar{n}_{1h}n_{2h}(e^{i(\xi_1-\xi_2)}e^{-i\omega\eta_-} - 1)], \tag{B1}$$

$$Z_{M,\rm CAR}(\xi_1+\xi_2) = p_{M,\rm CAR} + \mathcal{T}_{M,\rm CAR}[n_{1e}\bar{n}_{2h}(e^{i(\xi_1+\xi_2)}e^{i\omega\eta_-} - 1) + \bar{n}_{1e}n_{2h}e^{-i(\xi_1+\xi_2)}e^{-i\omega\eta_-} - 1)]$$
$$+ \bar{\mathcal{T}}_{M,\rm CAR}[n_{1h}\bar{n}_{2e}(e^{-i(\xi_1+\xi_2)}e^{i\omega\eta_-} - 1) + \bar{n}_{1h}n_{2e}(e^{i(\xi_1+\xi_2)}e^{-i\omega\eta_-} - 1)], \tag{B2}$$

$$Z_{M,\mathrm{LAR}}(\xi_1,\xi_2) = p_{M,\mathrm{LAR}}\{1+\mathcal{T}_{M,\mathrm{LAR},1}[n_{1e}\bar{n}_{1h}(e^{2i\xi_1}-1)+\bar{n}_{1e}n_{1h}(e^{-2i\xi_1}-1)]\} \times\{1+\mathcal{T}_{M,\mathrm{LAR},2}[n_{2e}\bar{n}_{2h}(e^{2i\xi_2}-1)+\bar{n}_{2e}n_{2h}(e^{-2i\xi_2}-1)]\}. \tag{B3}$$

The reflection and transmission coefficients are given by

$$\mathcal{T}_{M,\mathrm{NT}} = \bar{\mathcal{T}}_{M,\mathrm{NT}} = \mathcal{T}_{M,\mathrm{CAR}} = \bar{\mathcal{T}}_{M,\mathrm{CAR}} = \frac{4\Gamma_1\Gamma_2\epsilon_M^2}{\left(4\Gamma_1^2+\omega^2\right)\left(4\Gamma_2^2+\omega^2\right)+\epsilon_M^2\left(8\Gamma_1\Gamma_2+\epsilon_M^2-2\omega^2\right)},$$

$$\mathcal{T}_{M,\mathrm{LAR},\alpha} = \frac{4\Gamma_\alpha^2}{4\Gamma_\alpha^2+\omega^2},$$

$$p_{M,\mathrm{LAR}} = \frac{\left(4\Gamma_1^2+\omega^2\right)\left(4\Gamma_2^2+\omega^2\right)}{\left(4\Gamma_1^2+\omega^2\right)\left(4\Gamma_2^2+\omega^2\right)+\epsilon_M^2\left(8\Gamma_1\Gamma_2+\epsilon_M^2-2\omega^2\right)},$$

$$p_{M,\mathrm{NT}}+p_{M,\mathrm{CAR}} = \frac{\epsilon_M^2\left(8\Gamma_1\Gamma_2+\epsilon_M^2-2\omega^2\right)}{\left(4\Gamma_1^2+\omega^2\right)\left(4\Gamma_2^2+\omega^2\right)+\epsilon_M^2\left(8\Gamma_1\Gamma_2+\epsilon_M^2-2\omega^2\right)}.$$

We assume the effective coupling strengths are equal $\Gamma_1=\Gamma_2=\Gamma$. The particle currents from the left and right reservoirs are

$$J_1^N = \int\frac{d\omega}{2\pi}\frac{4\Gamma^2(n_{1e}\bar{n}_{1h}-n_{1h}\bar{n}_{1e})\left(4\Gamma^2+\epsilon_M^2+\omega^2\right)}{\left(4\Gamma^2+\omega^2\right)^2+(8\Gamma^2-2\omega^2)\epsilon_M^2+\epsilon_M^4} = \int\frac{d\omega}{2\pi}\,\mathbb{T}_N(\omega)(n_{1e}-n_{1h}), \tag{B4}$$

$$J_2^N = \int\frac{d\omega}{2\pi}\frac{4\Gamma^2(n_{2e}\bar{n}_{2h}-n_{2h}\bar{n}_{2e})\left(4\Gamma^2+\epsilon_M^2+\omega^2\right)}{\left(4\Gamma^2+\omega^2\right)^2+(8\Gamma^2-2\omega^2)\epsilon_M^2+\epsilon_M^4} = \int\frac{d\omega}{2\pi}\,\mathbb{T}_N(\omega)(n_{2e}-n_{2h}), \tag{B5}$$

where the transmission coefficient is

$$\mathbb{T}_N(\omega) = p_{M,\mathrm{LAR}}\mathcal{T}_{M,\mathrm{LAR}}+\mathcal{T}_{M,\mathrm{NT}} = \frac{4\Gamma^2\left(4\Gamma^2+\epsilon_M^2+\omega^2\right)}{\left(4\Gamma^2+\omega^2\right)^2+(8\Gamma^2-2\omega^2)\epsilon_M^2+\epsilon_M^4}.$$

The energy currents from the left and the right reservoirs are

$$\begin{aligned} J_1^E &= \int\frac{d\omega}{2\pi}\omega\frac{4\Gamma^2\omega\epsilon_M^2(n_{1e}+n_{1h}-n_{2e}-n_{2h})}{\left(4\Gamma^2+\omega^2\right)^2+(8\Gamma^2-2\omega^2)\epsilon_M^2+\epsilon_M^4} = \int\frac{d\omega}{2\pi}\,2\omega\mathbb{T}_E(\omega)(n_{1e}-n_{2e}),\\ J_2^E &= \int\frac{d\omega}{2\pi}\frac{4\Gamma^2\omega\epsilon_M^2(-n_{1e}-n_{1h}+n_{2e}+n_{2h})}{\left(4\Gamma^2+\omega^2\right)^2+(8\Gamma^2-2\omega^2)\epsilon_M^2+\epsilon_M^4} = \int\frac{d\omega}{2\pi}\,2\omega\mathbb{T}_E(\omega)(n_{2e}-n_{1e}), \end{aligned} \tag{B6}$$

with

$$\mathbb{T}_E(\omega) = \mathcal{T}_{M,\mathrm{NT}} = \frac{4\Gamma^2\epsilon_M^2}{\left(4\Gamma^2+\omega^2\right)^2+(8\Gamma^2-2\omega^2)\epsilon_M^2+\epsilon_M^4}.$$

The net effect of the NT and the CAR in the particle current J_α^N is to convert an electron in the left reservoir to an hole in the same reservoir. It can be seen by considering current $j(\omega)$ through a single channel ω. From the MGF Eqs. (B1) and (B2), the current components for a single channel ω from NT and CAR are

$$\begin{aligned} j_{\mathrm{NT}}(\omega) &\equiv \mathcal{T}_{M,\mathrm{NT}}(n_{1e}-n_{2e})-\bar{\mathcal{T}}_{M,\mathrm{NT}}(n_{1h}-n_{2h}),\\ j_{\mathrm{CAR}}(\omega) &\equiv \mathcal{T}_{M,\mathrm{CAR}}(n_{1e}-n_{2h})-\bar{\mathcal{T}}_{M,\mathrm{CAR}}(n_{1h}-n_{2e}). \end{aligned}$$

Since $\mathcal{T}_{M,\mathrm{NT}},=\bar{\mathcal{T}}_{M,\mathrm{NT}}=\mathcal{T}_{M,\mathrm{CAR}}=\bar{\mathcal{T}}_{M,\mathrm{CAR}}$, we have $j_{\mathrm{NT}}+j_{\mathrm{CAR}}=2\mathcal{T}_{M,\mathrm{NT}}(n_{1e}-n_{1h})$, which indicates the whole process is equivalent to a LAR. Again, we see that $J_1^N\neq J_2^N$ generally and $J_1^E=-J_2^E$. Previously, some studies, e.g., Refs. [81,82], incorrectly use the Landauer-Büttiker formula of a two-terminal system, instead of that of a three-terminal system, such as Eqs. (3) and (4) in Ref. [81] (in our notation)

$$J_1^N = \int\frac{d\omega}{2\pi}\,\mathbb{T}_N(\omega)[n_{1e}(\omega)-n_{2e}(\omega)], \tag{B7}$$

$$J_1^E = \int\frac{d\omega}{2\pi}\,\omega\mathbb{T}_N(\omega)[n_{1e}(\omega)-n_{2e}(\omega)]. \tag{B8}$$

The above expression of particle current Eq. (B7) only take the NT into account and neglect other two Andreev reflection processes, compared to Eq. (B4). That is why the above expressions of current gives half the quantized electrical conductance e^2/h (the correct one is $2e^2/h$). The expression of energy current Eq. (B8) is also incorrect in the transmission term $\mathbb{T}_N(\omega)$ compared to Eq. (B6), because $\mathbb{T}_N(\omega)$ incorrectly includes contributions from LAR which is not involved in the energy transport.

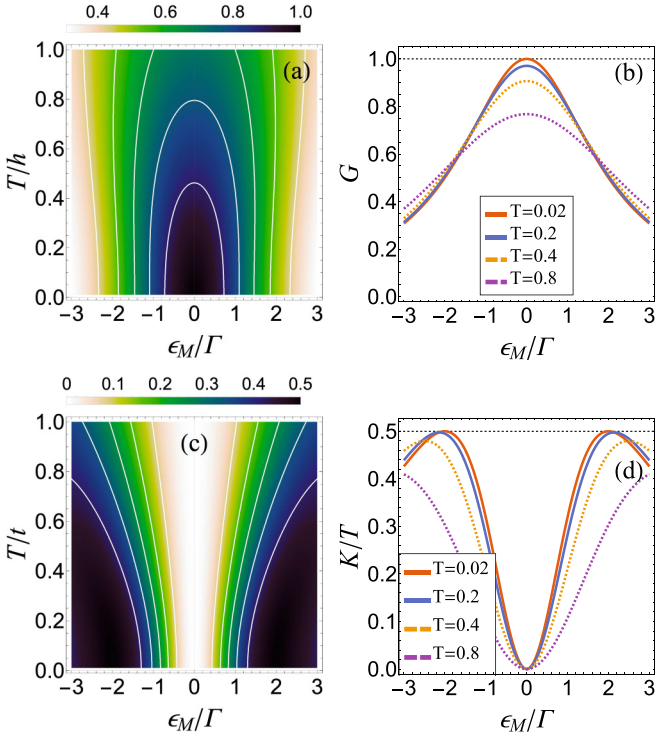

FIG. 7. The electrical conductance G_{11} in units of $2e^2/h$ and thermal conductance K/T in units of $\pi^2 k_B^2/3h$ for two MZMs. The coupling strength is set to $\Gamma = 1$. (a) Electrical conductance G_{11} as a function of the gap ϵ_M/Γ and the temperature T. (b) Cross sections of the electrical conductance at various temperatures $T = 0.02, 0.2, 0.4$, and 0.8. (c) Thermal conductance K/T as a function of the gap ϵ_M/Γ and the temperature T. (d) Cross sections of the thermal conductance at various temperatures $T = 0.02$, 0.2, 0.4, and 0.8.

1. Linear response regime

In the framework of the three-terminal system, the linear response matrix for two MZMs reads

$$L = \begin{pmatrix} L_{1,1} & 0 & 0 \\ 0 & L_{2,2} & 0 \\ 0 & 0 & L_{E,E} \end{pmatrix},$$

with

$$L_{1,1} = L_{2,2} = \int \frac{d\omega}{2\pi}\, \mathbb{T}_N(\omega) \frac{1}{2\cosh^2 \frac{\beta_2\omega}{2}},$$
$$L_{E,E} = \int \frac{d\omega}{2\pi}\, 2\omega^2 \mathbb{T}_E(\omega) \frac{1}{4\cosh^2 \frac{\beta_2\omega}{2}}. \tag{B9}$$

The electrical conductance is

$$G = \frac{e^2}{T}\begin{pmatrix} L_{1,1} & 0 \\ 0 & L_{2,2} \end{pmatrix},$$

which shows that there is no nonlocal conductance. The Seebeck coefficients are all zero. Thermal conductance is given by

$$K = \frac{1}{T^2} L_{E,E}.$$

In Fig. 7, we plot $K(\epsilon_M, T)$ and $G(\epsilon_M, T)$. The behavior of G is consistent with previous studies: it is quantized at $2e^2/h$ at zero gap $\epsilon_M = 0$ at low temperature. Nevertheless, the thermal conductance differs substantially from previous studies. It vanishes at zero gap regardless of the temperature and increases to the maximum at finite gap. Interestingly, the maximum value of K/T is about half-thermal conductance quantum $(1/2)\pi^2 k_B^2/3h$. As the temperature increases, the quantization is smeared out gradually. In the following, we demonstrate that the quantization of K/T is in fact exact. We measure the energy in the unit of T, i.e., we rescale $\omega \to \beta\omega$, $\Gamma \to \beta\Gamma$, $\epsilon_M \to \beta\epsilon_M$. Then K can be written as

$$K = T \int \frac{d\omega}{2\pi}\, 2\omega^2 \mathbb{T}_E(\omega) \frac{1}{4\cosh^2 \frac{\omega}{2}}.$$

The integral reaches its maximum in the limit $\Gamma/T \to \infty$ and $\epsilon_M/T \to \infty$ (zero-temperature limit). In this limit, we can approximate the integrand $\mathbb{T}_E(\omega) \approx \mathbb{T}_E(0)$ and carry out the integral

$$K/T = \mathbb{T}_E(0) \int \frac{d\omega}{2\pi} \frac{\omega^2}{2\cosh^2 \omega/2} = \frac{\pi}{3}\mathbb{T}_E(0)$$
$$= \frac{\pi}{3} \frac{4\Gamma^2\epsilon_M^2}{\left(4\Gamma^2 + \epsilon_M^2\right)^2} \leqslant \frac{\pi}{12} = \frac{1}{2}\frac{\pi^2 k_B^2}{3h},$$

where the equality is achieved at $\epsilon_M/\Gamma = 2$ and we resort to SI unit in the last equality. We show K/T as a function of Γ/T and ϵ_M/T in Fig. 8.

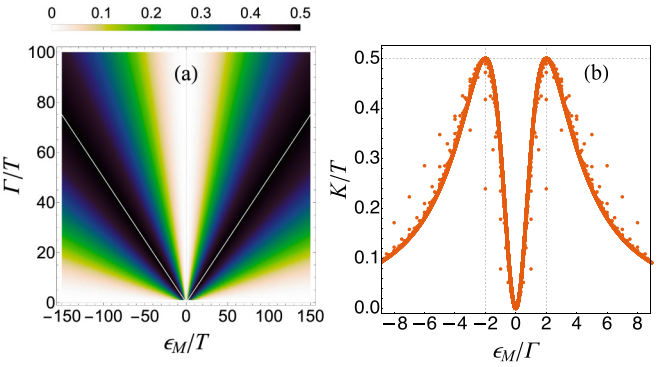

FIG. 8. (a) The thermal conductance K/T in units of $\pi^2 k_B^2/3h$ as a function of Γ/T and ϵ_M/T. The solid line is $2\Gamma = \epsilon_M$. (b) The thermal conductance K/T as a function of ϵ_M/Γ at $T = 0.02$. The maximum of K/T is half of a thermal conductance quantum $\pi^2 k_B^2/6h$, which is obtained in the zero-temperature limit $\epsilon_M/T \to \infty$, $\Gamma/T \to \infty$, and $\epsilon_M/\Gamma = 2$. The points deviating from the red curve in panel (b) correspond to small ϵ_M and small Γ.

2. Demonstration of the response relation

The explicit expression of the currents can give us some insight about the response coefficients. The occupation number

$$n_{1e}(\omega) - n_{1h}(\omega) = \frac{\sinh A_1}{\cosh\left[(\beta_2 - A_E)\omega\right] + \cosh A_1} \tag{B10}$$

is an odd function of A_1, thus all responses coefficients associated with even power terms of $A_1 = \beta_1\mu_1$ vanishes. Equation (B10) is also an even function of ω. Differentiating it with respect to $A_E = \beta_2 - \beta_1$ will not change the parity of

Eq. (B10). So the responses coefficients only associated with odd powers of A_1 are nonzero. Similar consideration applies to J_2^N. Since J_2^N does not depend on A_E, the response coefficients of J_2^N are diagonal. In the following, we demonstrate the validity of the nonlinear response relation

$$M_{i,jk} = \left(\frac{\partial D_{ij}}{\partial A_k} + \frac{\partial D_{ik}}{\partial A_j}\right)\Big|_{\boldsymbol{A}=0}$$

for $i = 1$ in the two MZMs model. Other cases can be checked similarly. From the expression of currents Eqs. (B4) and (B5), the only nonzero second-order response coefficient is

$$M_{1,1E} = M_{1,31} = \int \frac{d\omega}{2\pi}\, 2\omega \mathbb{T}_N p_0(1-p_0)(1-2p_0),$$

where $p_0 = 1/(e^{\beta_2\omega}+1)$. The current noises D_{1j} are

$$D_{11}(\boldsymbol{A}) = \frac{1}{2}\int \frac{d\omega}{2\pi}\big[\mathcal{T}_{M,\mathrm{NT}}(n_{1e}\bar{n}_{2e} + \bar{n}_{1e}n_{2e} + n_{1e}\bar{n}_{2h} + \bar{n}_{1e}n_{2h}) + 2p_{M,\mathrm{LAR}}\mathcal{T}_{M,\mathrm{LAR},1}(n_{1e}\bar{n}_{1h} + \bar{n}_{1e}n_{1h}) - \big(j_1^N\big)^2\big],$$

$$D_{12}(\boldsymbol{A}) = \frac{1}{2}\int \frac{d\omega}{2\pi}\big[\mathcal{T}_{M,\mathrm{NT}}(-n_{1e}\bar{n}_{2e} - \bar{n}_{1e}n_{2e} + n_{1e}\bar{n}_{2h} + \bar{n}_{1e}n_{2h}) + 2p_{M,\mathrm{LAR}}\mathcal{T}_{M,\mathrm{LAR},1}\mathcal{T}_{M,\mathrm{LAR},2}(n_{1e}-n_{1h})(n_{2e}-n_{2h}) - j_1^N j_2^N\big],$$

$$D_{1E}(\boldsymbol{A}) = \frac{1}{2}\int \frac{d\omega}{2\pi}\omega\big[\mathcal{T}_{M,\mathrm{NT}}(n_{1e}\bar{n}_{2e} + \bar{n}_{1e}n_{2e} + n_{1e}\bar{n}_{2h} + \bar{n}_{1e}n_{2h}) - j_1^N j_1^E\big].$$

At zero affinity, they reduce to

$$D_{11}(\boldsymbol{A}=0) = \int \frac{d\omega}{2\pi}\, 2\mathbb{T}_N p_0(1-p_0) = L_{1,1} = L_{2,2},$$

$$D_{1E}(\boldsymbol{A}=0) = \int \frac{d\omega}{2\pi}\, 2\omega\mathbb{T}_E p_0(1-p_0) = L_{1,E},$$

$$D_{12}(\boldsymbol{A}=0) = 0,$$

as expected. The derivatives of current noise D_{1i} at zero affinities are

$$\frac{\partial D_{1i}}{\partial A_j} = \int \frac{d\omega}{2\pi}\, p_0(1-p_0)(1-2p_0)\begin{pmatrix} 0 & 0 & \omega(\mathcal{T}_{M,\mathrm{NT}} + 2p_{M,\mathrm{LAR}}\mathcal{T}_{M,\mathrm{LAR},1}) \\ 0 & 0 & 0 \\ \omega\mathcal{T}_{M,\mathrm{NT}} & 0 & 0 \end{pmatrix}.$$

The symmetric sum of $D_{1j,k}$ is

$$\frac{\partial D_{1i}}{\partial A_j} + \frac{\partial D_{1j}}{\partial A_i} = \begin{pmatrix} 0 & 0 & D_{11,E} + D_{1E,1} \\ 0 & 0 & 0 \\ D_{1E,1} + D_{11,E} & 0 & 0 \end{pmatrix}.$$

In comparison with the expression of $M_{1,jk}$ we verify Eq. (A15) in the two Majorana modes system

$$M_{1,jk} = \left(\frac{\partial D_{1j}}{\partial A_k} + \frac{\partial D_{1k}}{\partial A_j}\right)\Big|_{\boldsymbol{A}=0}.$$

[1] L. Onsager, Phys. Rev. **37**, 405 (1931).
[2] L. Onsager, Phys. Rev. **38**, 2265 (1931).
[3] H. B. G. Casimir, Rev. Mod. Phys. **17**, 343 (1945).
[4] H. B. Callen and T. A. Welton, Phys. Rev. **83**, 34 (1951).
[5] D. J. Evans, E. G. D. Cohen, and G. P. Morriss, Phys. Rev. Lett. **71**, 2401 (1993).
[6] D. J. Evans and D. J. Searles, Phys. Rev. E **50**, 1645 (1994).
[7] G. Gallavotti and E. G. D. Cohen, J. Stat. Phys. **80**, 931 (1995).
[8] G. Gallavotti and E. G. D. Cohen, Phys. Rev. Lett. **74**, 2694 (1995).
[9] J. Kurchan, J. Phys. A: Math. Gen. **31**, 3719 (1998).
[10] C. Maes, J. Stat. Phys. **95**, 367 (1999).
[11] J. L. Lebowitz and H. Spohn, J. Stat. Phys. **95**, 333 (1999).
[12] M. Esposito, U. Harbola, and S. Mukamel, Rev. Mod. Phys. **81**, 1665 (2009).
[13] M. Campisi, P. Hänggi, and P. Talkner, Rev. Mod. Phys. **83**, 771 (2011).
[14] C. Jarzynski, Annu. Rev. Condens. Matter Phys. **2**, 329 (2011).
[15] U. Seifert, Rep. Prog. Phys. **75**, 126001 (2012).
[16] K. Saito and Y. Utsumi, Phys. Rev. B **78**, 115429 (2008).
[17] D. Andrieux and P. Gaspard, Phys. Rev. Lett. **100**, 230404 (2008).
[18] D. Andrieux, P. Gaspard, T. Monnai, and S. Tasaki, New J. Phys. **11**, 043014 (2009).
[19] P. Gaspard, New J. Phys. **15**, 115014 (2013).
[20] J. Gu and P. Gaspard, Phys. Rev. E **99**, 012137 (2019).
[21] M. Barbier and P. Gaspard, Phys. Rev. E **102**, 022141 (2020).
[22] J. Gu and P. Gaspard, J. Stat. Mech.: Theory Exp. (2020) 103206.

[23] Y.-X. Wu, J. Gu, and H. T. Quan, Phys. Rev. E **106**, 014154 (2022).

[24] C. Jarzynski and D. K. Wójcik, Phys. Rev. Lett. **92**, 230602 (2004).

[25] F. Zhang and H. T. Quan, Phys. Rev. E **103**, 032143 (2021).

[26] Y. Oreg, G. Refael, and F. von Oppen, Phys. Rev. Lett. **105**, 177002 (2010).

[27] R. M. Lutchyn, J. D. Sau, and S. Das Sarma, Phys. Rev. Lett. **105**, 077001 (2010).

[28] G.-J. Qiao, S.-W. Li, and C. P. Sun, Phys. Rev. B **106**, 104517 (2022).

[29] V. Mourik, K. Zuo, S. M. Frolov, S. R. Plissard, E. P. A. M. Bakkers, and L. P. Kouwenhoven, Science **336**, 1003 (2012).

[30] A. Das, Y. Ronen, Y. Most, Y. Oreg, M. Heiblum, and H. Shtrikman, Nat. Phys. **8**, 887 (2012).

[31] M. T. Deng, C. L. Yu, G. Y. Huang, M. Larsson, P. Caroff, and H. Q. Xu, Nano Lett. **12**, 6414 (2012).

[32] S. Nadj-Perge, I. K. Drozdov, J. Li, H. Chen, S. Jeon, J. Seo, A. H. MacDonald, B. A. Bernevig, and A. Yazdani, Science **346**, 602 (2014).

[33] M. Valentini, F. P. naranda, A. Hofmann, M. Brauns, R. Hauschild, P. Krogstrup, P. San-Jose, E. Prada, R. Aguado, and G. Katsaros, Science **373**, 82 (2021).

[34] H. Pan, J. D. Sau, and S. Das Sarma, Phys. Rev. B **103**, 014513 (2021).

[35] J.-Y. Wang, N. van Loo, G. P. Mazur, V. Levajac, F. K. Malinowski, M. Lemang, F. Borsoi, G. Badawy, S. Gazibegovic, E. P. A. M. Bakkers, M. Quintero-Pérez, S. Heedt, and L. P. Kouwenhoven, Phys. Rev. B **106**, 075306 (2022).

[36] K. Flensberg, F. von Oppen, and A. Stern, Nat Rev Mater **6**, 944 (2021).

[37] A. Kamenev, *Field Theory of Non-Equilibrium Systems* (Cambridge University Press, Cambridge, UK, 2011).

[38] R. Shankar, *Quantum Field Theory and Condensed Matter: An Introduction* (Cambridge University Press, Cambridge, UK, 2017).

[39] J. Nilsson, A. R. Akhmerov, and C. W. J. Beenakker, Phys. Rev. Lett. **101**, 120403 (2008).

[40] K. T. Law, P. A. Lee, and T. K. Ng, Phys. Rev. Lett. **103**, 237001 (2009).

[41] In fact, the CAR occurs when the site number is even. If the site number is odd, then NT rather than CAR will occur.

[42] In fact, the number of sites should be larger than 3.

[43] A. D'Abbruzzo and D. Rossini, Phys. Rev. B **104**, 115139 (2021).

[44] N. Leumer, M. Grifoni, B. Muralidharan, and M. Marganska, Phys. Rev. B **103**, 165432 (2021).

[45] K. Flensberg, Phys. Rev. B **82**, 180516(R) (2010).

[46] D. Roy, C. J. Bolech, and N. Shah, Phys. Rev. B **86**, 094503 (2012).

[47] E. Prada, P. San-Jose, and R. Aguado, Phys. Rev. B **86**, 180503(R) (2012).

[48] R. J. Doornenbal, G. Skantzaris, and H. T. C. Stoof, Phys. Rev. B **91**, 045419 (2015).

[49] A. M. Lobos and S. D. Sarma, New J. Phys. **17**, 065010 (2015).

[50] A. Zazunov, R. Egger, and A. Levy Yeyati, Phys. Rev. B **94**, 014502 (2016).

[51] J. M. Bhat and A. Dhar, Phys. Rev. B **102**, 224512 (2020).

[52] N. Bondyopadhaya and D. Roy, J. Stat. Phys. **187**, 11 (2022).

[53] A. R. Akhmerov, J. P. Dahlhaus, F. Hassler, M. Wimmer, and C. W. J. Beenakker, Phys. Rev. Lett. **106**, 057001 (2011).

[54] H. Li and Y. Y. Zhao, J. Phys.: Condens. Matter **29**, 465001 (2017).

[55] S. Verma and A. Singh, J. Phys.: Condens. Matter **34**, 155601 (2022).

[56] G. C. Ménard, G. L. R. Anselmetti, E. A. Martinez, D. Puglia, F. K. Malinowski, J. S. Lee, S. Choi, M. Pendharkar, C. J. Palmstrøm, K. Flensberg, C. M. Marcus, L. Casparis, and A. P. Higginbotham, Phys. Rev. Lett. **124**, 036802 (2020).

[57] H. Pan, C.-X. Liu, M. Wimmer, and S. Das Sarma, Phys. Rev. B **103**, 214502 (2021).

[58] A. Maiani, M. Geier, and K. Flensberg, Phys. Rev. B **106**, 104516 (2022).

[59] R. S. Whitney, R. Sánchez, and J. Splettstoesser, Quantum thermodynamics of nanoscale thermoelectrics and electronic devices, in *Thermodynamics in the Quantum Regime: Fundamental Aspects and New Directions*, edited by F. Binder, L. A. Correa, C. Gogolin, J. Anders, and G. Adesso (Springer International Publishing, Cham, 2018), pp. 175–206.

[60] F. Mazza, R. Bosisio, G. Benenti, V. Giovannetti, R. Fazio, and F. Taddei, New J. Phys. **16**, 085001 (2014).

[61] S. J. Blundell and K. M. Blundell, *Concepts in Thermal Physics* (Oxford University Press, Oxford, UK, 2010).

[62] J. S. Lim, R. López, and L. Serra, New J. Phys. **14**, 083020 (2012).

[63] The relation between Γ_α and $\lambda_{\alpha j}$ can be found in our previous paper [25].

[64] O. Entin-Wohlman, Y. Imry, and A. Aharony, Phys. Rev. B **82**, 115314 (2010).

[65] J.-H. Jiang, O. Entin-Wohlman, and Y. Imry, Phys. Rev. B **85**, 075412 (2012).

[66] J.-H. Jiang, O. Entin-Wohlman, and Y. Imry, New J. Phys. **15**, 075021 (2013).

[67] J.-H. Jiang, M. Kulkarni, D. Segal, and Y. Imry, Phys. Rev. B **92**, 045309 (2015).

[68] H. Thierschmann, R. Sánchez, B. Sothmann, F. Arnold, C. Heyn, W. Hansen, H. Buhmann, and L. W. Molenkamp, Nat. Nanotechnol. **10**, 854 (2015).

[69] R. Sánchez and M. Büttiker, Phys. Rev. B **83**, 085428 (2011).

[70] G. Jaliel, R. K. Puddy, R. Sánchez, A. N. Jordan, B. Sothmann, I. Farrer, J. P. Griffiths, D. A. Ritchie, and C. G. Smith, Phys. Rev. Lett. **123**, 117701 (2019).

[71] S. Dorsch, A. Svilans, M. Josefsson, B. Goldozian, M. Kumar, C. Thelander, A. Wacker, and A. Burke, Nano Lett. **21**, 988 (2021).

[72] Z. Cao, T.-F. Fang, L. Li, and H.-G. Luo, Appl. Phys. Lett. **107**, 212601 (2015).

[73] R. Sánchez, P. Burset, and A. L. Yeyati, Phys. Rev. B **98**, 241414(R) (2018).

[74] R. Hussein, M. Governale, S. Kohler, W. Belzig, F. Giazotto, and A. Braggio, Phys. Rev. B **99**, 075429 (2019).

[75] N. S. Kirsanov, Z. B. Tan, D. S. Golubev, P. J. Hakonen, and G. B. Lesovik, Phys. Rev. B **99**, 115127 (2019).

[76] D. S. Fisher and P. A. Lee, Phys. Rev. B **23**, 6851 (1981).

[77] G. Meurant, SIAM J. Matrix Anal. Appl. **13**, 707 (1992).
[78] I. Rungger and S. Sanvito, Phys. Rev. B **78**, 035407 (2008).
[79] M. G. Reuter and J. C. Hill, Comput. Sci. Discovery **5**, 014009 (2012).
[80] J. Meair and P. Jacquod, J. Phys.: Condens. Matter **25**, 082201 (2013).
[81] R. López, M. Lee, L. Serra, and J. S. Lim, Phys. Rev. B **89**, 205418 (2014).
[82] J. P. Ramos-Andrade, O. Ávalos-Ovando, P. A. Orellana, and S. E. Ulloa, Phys. Rev. B **94**, 155436 (2016).